Ontario

We are committed to providing accessible customer service.
If you need accessible formats or communications supports, please contact us.

Nous tenons à améliorer l'accessibilité des services à la clientèle.
Si vous avez besoin de formats accessibles ou d'aide à la communication, veuillez nous contacter.

Reprocessed Data Assessment Report

Gowan Project, Ontario, Canada

Prepared for:

Fortune Nickel & Gold Inc.

Attention To: Paul Riss
800 Westchester Ave, 10573
Rye Brook, New York, USA

Mining Claims:

522431, 522432, 522433, 522434, 522435, 522436, 522437, 522438, 576202, 576203, 576204, 576205, 576206, 576207, 576331, 576332, 576333, 576334, 576335, 576336, 576337, 576484, 576485, 576486, 576487, 576488, 576591, 576592, 576593, 576594, 576595, 576596, 576597, 576598, 576599, 576600, 613708, 613709, 613710, 613711, 613712, 613713, 613714, 613715, 613716, 613717, 613718, 613719, 613720, 613721, 613722, 613723, 613724, 613725, 613726, 613727, 613728, 613729, 613730, 613731, 613732, 613733, 613734, 613735, 613736, 613737, 613738, 613739, 613740, 613741, 613742, 613743, 613744, 613745, 613746, 613747, 613748, 613749, 613750, 613751, 613752, 613753, 613754, 613755, 613756, 613757, 613758, 613759, 613760, 613761, 613762, 613763, 613764, 613765, 613766, 613767, 613768, 613769, 613770, 613771, 613772, 613773

NTS 042A/11
NAD83 / UTM Zone 17N

Prepared By:

Axiom Exploration Group Ltd.

Suite 101 - 3239 Faithfull Avenue
Saskatoon, SK, Canada

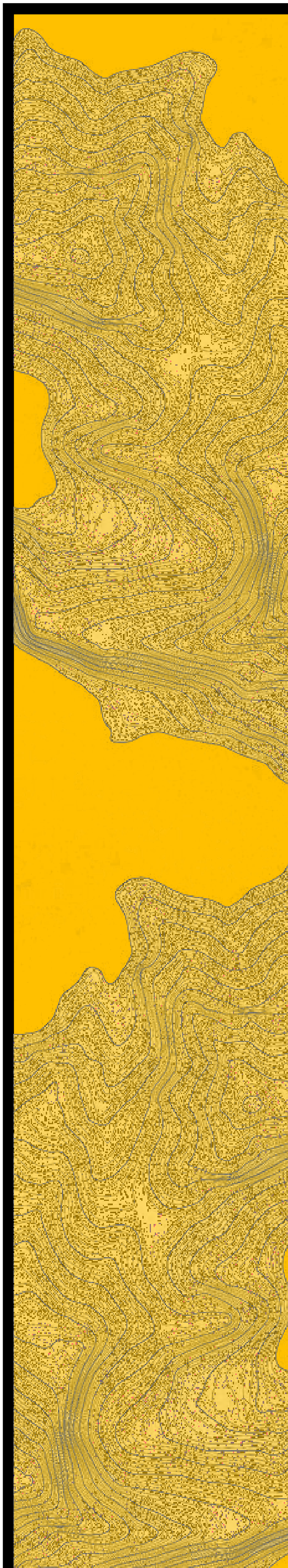

February 17th, 2023

Jeffery Balas, G.I.T.
Darren Slugoski, P. Geo

TABLE OF CONTENTS

LIST OF FIGURES

LIST OF TABLES

1. SUMMARY

Fortune Nickel & Gold Inc. ('Fortune') engaged Axiom Exploration Group Ltd. ('Axiom') of Saskatoon, Saskatchewan to complete an assessment report for recently acquired Synthetic Aperture Radar ('SAR') and Sentinel & Aster multispectral data for the Gowan project area, located approximately 25 kilometres northeast from the city of Timmins in Ontario.

The Gowan property ('the Property') was acquired based on the Client's ongoing regional compilation to target the most prospective areas for new nickel, gold, and base metal mines. To move the project forward, the Fortune commenced detailed analysis on remotely sensed satellite survey data from the Property. The survey data was acquired and analyzed by Axiom's Applied Analytics division specialists.

A total study area of approximately 40 km^2 was surveyed between January 4, 2023 to January 30, 2023. This work included collecting, processing, analyzing, and interpreting data from SAR as well as multispectral data from Sentinel & Aster satellites. Along with the interpretations, a digital elevation model (DEM) was provided to the Client.

The satellite analysis survey was successful in identifying both regional and local structures in the project area. Iron, alteration, and other anomalies outlined in the report can potentially be used to assist in identifying attractive areas for future mineral exploration targets and mapping work on the Property.

Recommendations for future work are provided in section 12 of this assessment report.

The satellite data acquisition & analysis logistics report is attached in Appendix A. This includes the final maps for Structural Analysis, Iron Index, Gossan, Soil Vegetation Index ('SVI'), Alunite-Kaolinite-Pyrophyllite index, Alteration with Fault Targets, Sentinel 2 Ferric Iron, and Rose Diagram from Structural Analysis.

Table 1: Project Personnel & Support Staff

Data Acquisition & Analysis	Pieter Du Plessis
Data Acquisition & Analysis	Thomas Stanley-Jones
Technical Report Drafting	Jeffery Balas
Technical Report Supervisor	Darren Slugoski

2. INTRODUCTION & PROPERTY OVERVIEW

The Gowan project is comprised of 102 single cell mining claims, totalling 2176.33 hectares, which at the time of writing, are 100% owned by Fortune Nickel & Gold Inc., a wholly owned subsidiary of Here to Serve Holding Corp (Table 3).

The property occupies the National Topographic System (NTS) map sheets 042A/11. The Property claims are situated in the prolific Porcupine Mining Division. This area of Ontario has historically hosted several significant gold, nickel, copper, and zinc mines & prospects, and is located approximately 30 kilometres north from Glencore's Kidd Creek Mine and 15 kilometres north from Canada Nickel's Crawford Nickel-Cobalt Sulphide Project.

Historically, there are approximately 3150 m of diamond drill holes on the property within the claim boundaries which returned anomalous Ni, Cu, and Zn values (Skinner, 1973a; Ontario Drill Hole Database).

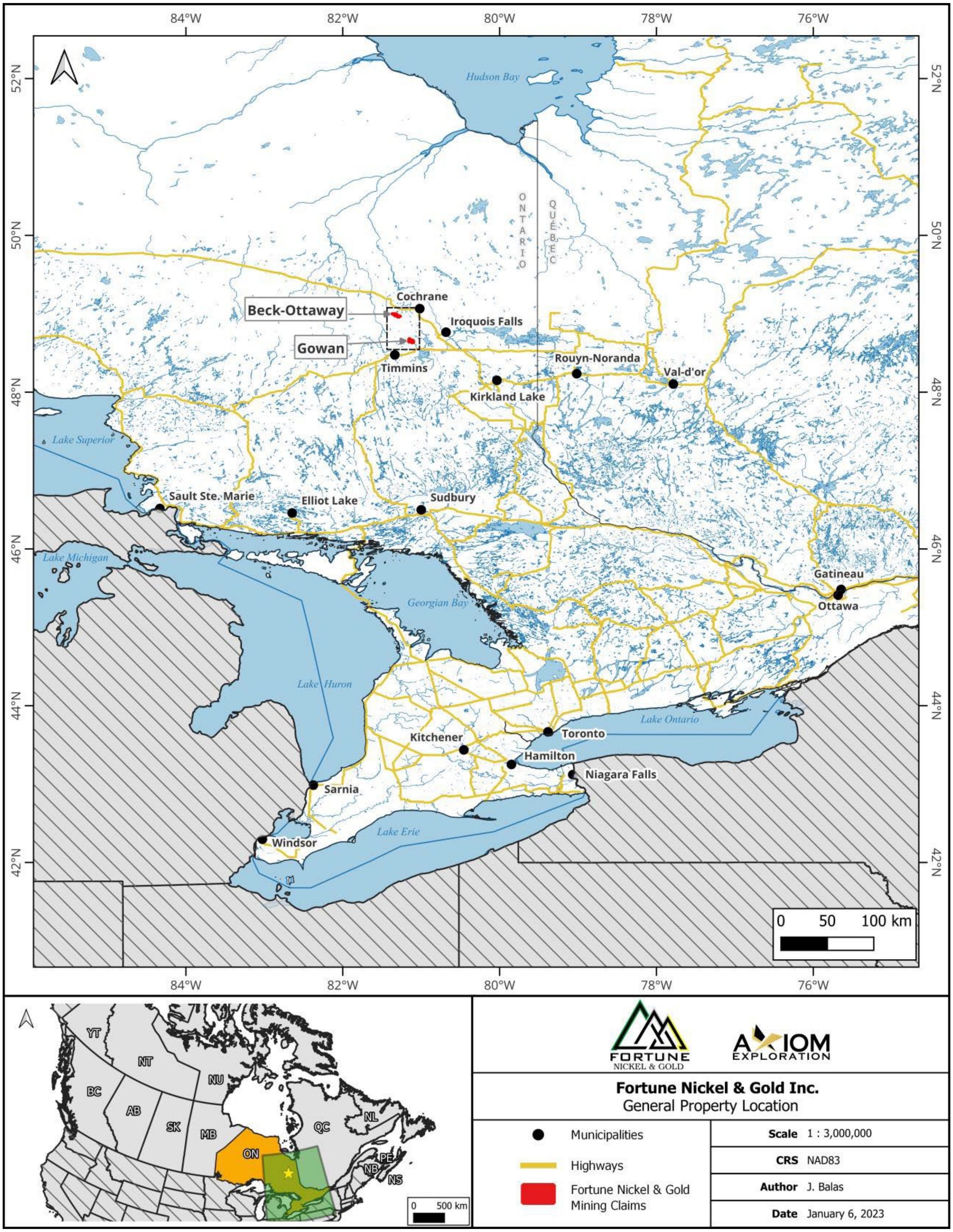

<u>Figure 1:</u> General property location. The box near Timmins shows the two project locations owned by Fortune Nickel & Gold Inc.

3. LOCATION & ACCESS

The Property is located approximately 25 kilometers northeast of the city of Timmins in northeastern Ontario. There are many developed prospects with provable resources & reserves as well as producing & past-producing mines within the vicinity of the project area, including Kidd Creek mine, which is approximately 15 kilometers to the west (Figure 1, Figure 2, Figure 3).

The Property currently does not have all-season road access directly to the property. The Property can be accessed by driving north on the Ice Chest Lake gravel road, and then using an all-terrain vehicle with amphibious capability due west (Geo-Environmental Site Report, Gowan Mining Claims, 2020).

There are many off-road vehicle trails throughout the property, but due to clay-rich soil conditions, the area is prone to flooding and standing water (Percival and Easton, 2007a). If a helicopter is to be used for an exploration program in the future, pads must first be built for suitable landing sites.

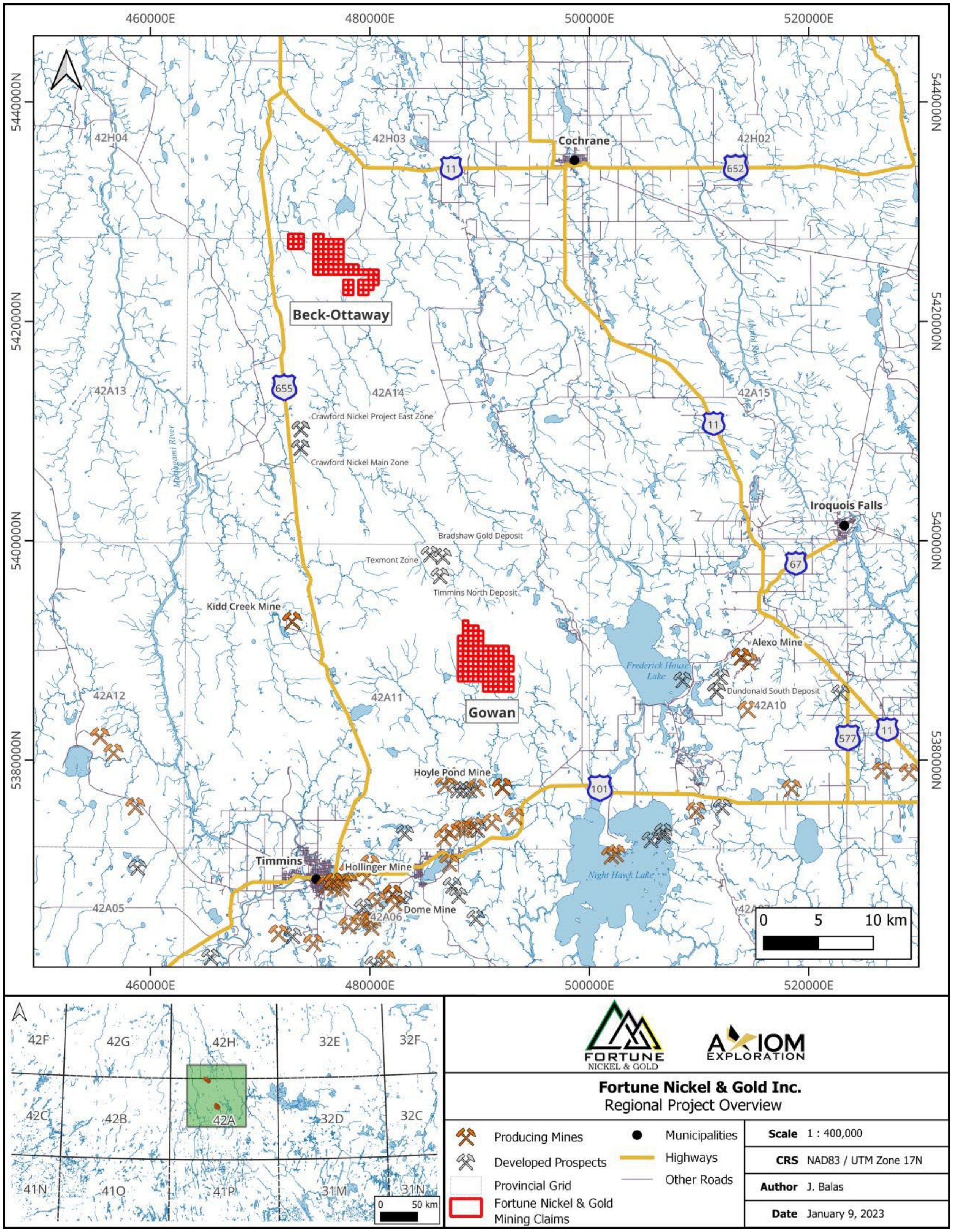

Figure 2: Regional Overview.

4. CLIMATE & PHYSIOGRAPHY

The property area is located within the Humid Mid-Boreal Ecoclimatic Region, which is characterized by warm and short summers, while winters are long, cold, and snowy (Ecoregions Working Group, 1989).

According to Environmental and Natural Resources Canada, temperatures in the region typically range from an average low of -23.0°C in January to an average high of +24.2°C in July. Average annual precipitation is 834.6 mm, with the highest levels being in the summer, while the average snowfall is 311.3 cm (Canadian Climate Normals 1981-2010 Station Data - Climate - Environment and Climate Change Canada).

The property is located within the northern boundary of the Kirkland Lake Ecodistrict (3E-6) of the Lake Abitibi Ecoregion within the Ontario Shield Ecozone. The physiography is characterized by mixed forests, glaciolacustrine deposits, and Precambrian bedrock (Wester et al.).

5. MINING CLAIMS & OWNERSHIP

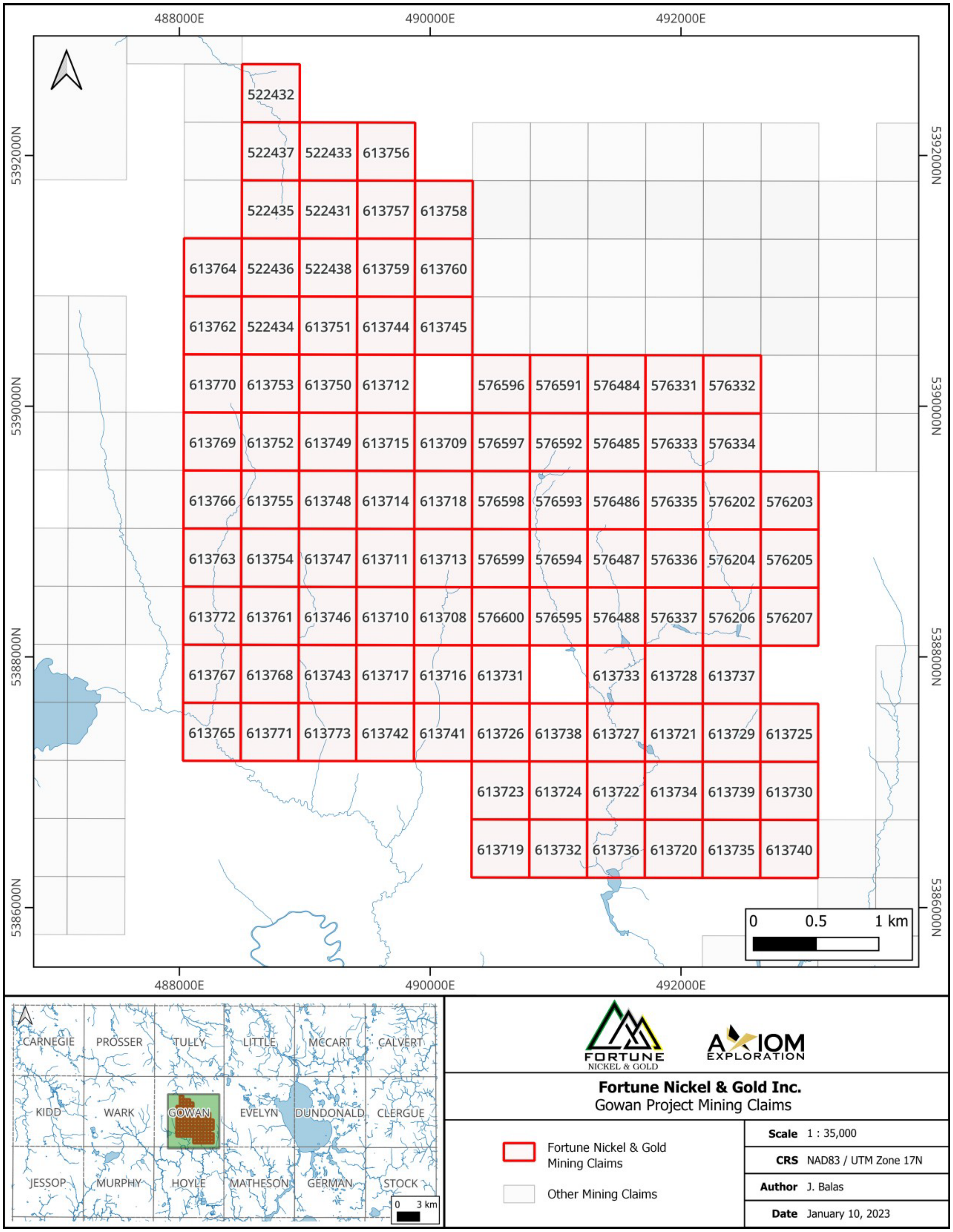

Figure 3: Mining Claim Map.

Table 2: **Mining Claim Information.**

Claim Number	Township	NTS Grid	Issue Date	Claim Due	Holder	Area (ha)
522431	GOWAN	42A11	2018-06-02	2023-06-02	(100) Fortune Nickel and Gold Inc.	21.33
522432	GOWAN	42A11	2018-06-02	2023-06-02	(100) Fortune Nickel and Gold Inc.	21.32
522433	GOWAN	42A11	2018-06-02	2023-06-02	(100) Fortune Nickel and Gold Inc.	21.32
522434	GOWAN	42A11	2018-06-02	2023-06-02	(100) Fortune Nickel and Gold Inc.	21.33
522435	GOWAN	42A11	2018-06-02	2023-06-02	(100) Fortune Nickel and Gold Inc.	21.33
522436	GOWAN	42A11	2018-06-02	2023-06-02	(100) Fortune Nickel and Gold Inc.	21.33
522437	GOWAN	42A11	2018-06-02	2023-06-02	(100) Fortune Nickel and Gold Inc.	21.32
522438	GOWAN	42A11	2018-06-02	2023-06-02	(100) Fortune Nickel and Gold Inc.	21.33
576202	GOWAN	42A11	2020-02-08	2023-02-08	(100) Fortune Nickel and Gold Inc.	21.34
576203	GOWAN	42A11	2020-02-08	2023-02-08	(100) Fortune Nickel and Gold Inc.	21.34
576204	GOWAN	42A11	2020-02-08	2023-02-08	(100) Fortune Nickel and Gold Inc.	21.34
576205	GOWAN	42A11	2020-02-08	2023-02-08	(100) Fortune Nickel and Gold Inc.	21.34
576206	GOWAN	42A11	2020-02-08	2023-02-08	(100) Fortune Nickel and Gold Inc.	21.34
576207	GOWAN	42A11	2020-02-08	2023-02-08	(100) Fortune Nickel and Gold Inc.	21.34
576331	GOWAN	42A11	2020-02-11	2023-02-11	(100) Fortune Nickel and Gold Inc.	21.33
576332	GOWAN	42A11	2020-02-11	2023-02-11	(100) Fortune Nickel and Gold Inc.	21.33
576333	GOWAN	42A11	2020-02-11	2023-02-11	(100) Fortune Nickel and Gold Inc.	21.33
576334	GOWAN	42A11	2020-02-11	2023-02-11	(100) Fortune Nickel and Gold Inc.	21.33
576335	GOWAN	42A11	2020-02-11	2023-02-11	(100) Fortune Nickel and Gold Inc.	21.34
576336	GOWAN	42A11	2020-02-11	2023-02-11	(100) Fortune Nickel and Gold Inc.	21.34
576337	GOWAN	42A11	2020-02-11	2023-02-11	(100) Fortune Nickel and Gold Inc.	21.34
576484	GOWAN	42A11	2020-02-12	2023-02-12	(100) Fortune Nickel and Gold Inc.	21.33
576485	GOWAN	42A11	2020-02-12	2023-02-12	(100) Fortune Nickel and Gold Inc.	21.33

576486	GOWAN	42A11	2020-02-12	2023-02-12	(100) Fortune Nickel and Gold Inc.	21.34
576487	GOWAN	42A11	2020-02-12	2023-02-12	(100) Fortune Nickel and Gold Inc.	21.34
576488	GOWAN	42A11	2020-02-12	2023-02-12	(100) Fortune Nickel and Gold Inc.	21.34
576591	GOWAN	42A11	2020-02-13	2023-02-13	(100) Fortune Nickel and Gold Inc.	21.33
576592	GOWAN	42A11	2020-02-13	2023-02-13	(100) Fortune Nickel and Gold Inc.	21.33
576593	GOWAN	42A11	2020-02-13	2023-02-13	(100) Fortune Nickel and Gold Inc.	21.34
576594	GOWAN	42A11	2020-02-13	2023-02-13	(100) Fortune Nickel and Gold Inc.	21.34
576595	GOWAN	42A11	2020-02-13	2023-02-13	(100) Fortune Nickel and Gold Inc.	21.34
576596	GOWAN	42A11	2020-02-13	2023-02-13	(100) Fortune Nickel and Gold Inc.	21.33
576597	GOWAN	42A11	2020-02-13	2023-02-13	(100) Fortune Nickel and Gold Inc.	21.33
576598	GOWAN	42A11	2020-02-13	2023-02-13	(100) Fortune Nickel and Gold Inc.	21.34
576599	GOWAN	42A11	2020-02-13	2023-02-13	(100) Fortune Nickel and Gold Inc.	21.34
576600	GOWAN	42A11	2020-02-13	2023-02-13	(100) Fortune Nickel and Gold Inc.	21.34
613708	GOWAN	42A11	2020-10-02	2023-10-02	(100) Fortune Nickel and Gold Inc.	21.34
613709	GOWAN	42A11	2020-10-02	2023-10-02	(100) Fortune Nickel and Gold Inc.	21.33
613710	GOWAN	42A11	2020-10-02	2023-10-02	(100) Fortune Nickel and Gold Inc.	21.34
613711	GOWAN	42A11	2020-10-02	2023-10-02	(100) Fortune Nickel and Gold Inc.	21.34
613712	GOWAN	42A11	2020-10-02	2023-10-02	(100) Fortune Nickel and Gold Inc.	21.33
613713	GOWAN	42A11	2020-10-02	2023-10-02	(100) Fortune Nickel and Gold Inc.	21.34
613714	GOWAN	42A11	2020-10-02	2023-10-02	(100) Fortune Nickel and Gold Inc.	21.34
613715	GOWAN	42A11	2020-10-02	2023-10-02	(100) Fortune Nickel and Gold Inc.	21.33
613716	GOWAN	42A11	2020-10-02	2023-10-02	(100) Fortune Nickel and Gold Inc.	21.34
613717	GOWAN	42A11	2020-10-02	2023-10-02	(100) Fortune Nickel and Gold Inc.	21.34
613718	GOWAN	42A11	2020-10-02	2023-10-02	(100) Fortune Nickel and Gold Inc.	21.34
613719	GOWAN	42A11	2020-10-02	2023-10-02	(100) Fortune Nickel and Gold Inc.	21.35

613720	GOWAN	42A11	2020-10-02	2023-10-02	(100) Fortune Nickel and Gold Inc.	21.35
613721	GOWAN	42A11	2020-10-02	2023-10-02	(100) Fortune Nickel and Gold Inc.	21.34
613722	GOWAN	42A11	2020-10-02	2023-10-02	(100) Fortune Nickel and Gold Inc.	21.34
613723	GOWAN	42A11	2020-10-02	2023-10-02	(100) Fortune Nickel and Gold Inc.	21.34
613724	GOWAN	42A11	2020-10-02	2023-10-02	(100) Fortune Nickel and Gold Inc.	21.34
613725	GOWAN	42A11	2020-10-02	2023-10-02	(100) Fortune Nickel and Gold Inc.	21.34
613726	GOWAN	42A11	2020-10-02	2023-10-02	(100) Fortune Nickel and Gold Inc.	21.34
613727	GOWAN	42A11	2020-10-02	2023-10-02	(100) Fortune Nickel and Gold Inc.	21.34
613728	GOWAN	42A11	2020-10-02	2023-10-02	(100) Fortune Nickel and Gold Inc.	21.34
613729	GOWAN	42A11	2020-10-02	2023-10-02	(100) Fortune Nickel and Gold Inc.	21.34
613730	GOWAN	42A11	2020-10-02	2023-10-02	(100) Fortune Nickel and Gold Inc.	21.34
613731	GOWAN	42A11	2020-10-02	2023-10-02	(100) Fortune Nickel and Gold Inc.	21.34
613732	GOWAN	42A11	2020-10-02	2023-10-02	(100) Fortune Nickel and Gold Inc.	21.35
613733	GOWAN	42A11	2020-10-02	2023-10-02	(100) Fortune Nickel and Gold Inc.	21.34
613734	GOWAN	42A11	2020-10-02	2023-10-02	(100) Fortune Nickel and Gold Inc.	21.34
613735	GOWAN	42A11	2020-10-02	2023-10-02	(100) Fortune Nickel and Gold Inc.	21.35
613736	GOWAN	42A11	2020-10-02	2023-10-02	(100) Fortune Nickel and Gold Inc.	21.35
613737	GOWAN	42A11	2020-10-02	2023-10-02	(100) Fortune Nickel and Gold Inc.	21.34
613738	GOWAN	42A11	2020-10-02	2023-10-02	(100) Fortune Nickel and Gold Inc.	21.34
613739	GOWAN	42A11	2020-10-02	2023-10-02	(100) Fortune Nickel and Gold Inc.	21.34
613740	GOWAN	42A11	2020-10-02	2023-10-02	(100) Fortune Nickel and Gold Inc.	21.35
613741	GOWAN	42A11	2020-10-02	2023-10-02	(100) Fortune Nickel and Gold Inc.	21.34
613742	GOWAN	42A11	2020-10-02	2023-10-02	(100) Fortune Nickel and Gold Inc.	21.34
613743	GOWAN	42A11	2020-10-02	2023-10-02	(100) Fortune Nickel and Gold Inc.	21.34
613744	GOWAN	42A11	2020-10-02	2023-10-02	(100) Fortune Nickel and Gold Inc.	21.33

613745	GOWAN	42A11	2020-10-02	2023-10-02	(100) Fortune Nickel and Gold Inc.	21.33
613746	GOWAN	42A11	2020-10-02	2023-10-02	(100) Fortune Nickel and Gold Inc.	21.34
613747	GOWAN	42A11	2020-10-02	2023-10-02	(100) Fortune Nickel and Gold Inc.	21.34
613748	GOWAN	42A11	2020-10-02	2023-10-02	(100) Fortune Nickel and Gold Inc.	21.34
613749	GOWAN	42A11	2020-10-02	2023-10-02	(100) Fortune Nickel and Gold Inc.	21.33
613750	GOWAN	42A11	2020-10-02	2023-10-02	(100) Fortune Nickel and Gold Inc.	21.33
613751	GOWAN	42A11	2020-10-02	2023-10-02	(100) Fortune Nickel and Gold Inc.	21.33
613752	GOWAN	42A11	2020-10-02	2023-10-02	(100) Fortune Nickel and Gold Inc.	21.33
613753	GOWAN	42A11	2020-10-02	2023-10-02	(100) Fortune Nickel and Gold Inc.	21.33
613754	GOWAN	42A11	2020-10-02	2023-10-02	(100) Fortune Nickel and Gold Inc.	21.34
613755	GOWAN	42A11	2020-10-02	2023-10-02	(100) Fortune Nickel and Gold Inc.	21.34
613756	GOWAN	42A11	2020-10-02	2023-10-02	(100) Fortune Nickel and Gold Inc.	21.32
613757	GOWAN	42A11	2020-10-02	2023-10-02	(100) Fortune Nickel and Gold Inc.	21.33
613758	GOWAN	42A11	2020-10-02	2023-10-02	(100) Fortune Nickel and Gold Inc.	21.33
613759	GOWAN	42A11	2020-10-02	2023-10-02	(100) Fortune Nickel and Gold Inc.	21.33
613760	GOWAN	42A11	2020-10-02	2023-10-02	(100) Fortune Nickel and Gold Inc.	21.33
613761	GOWAN	42A11	2020-10-02	2023-10-02	(100) Fortune Nickel and Gold Inc.	21.34
613762	GOWAN	42A11	2020-10-02	2023-10-02	(100) Fortune Nickel and Gold Inc.	21.33
613763	GOWAN	42A11	2020-10-02	2023-10-02	(100) Fortune Nickel and Gold Inc.	21.34
613764	GOWAN	42A11	2020-10-02	2023-10-02	(100) Fortune Nickel and Gold Inc.	21.33
613765	GOWAN	42A11	2020-10-02	2023-10-02	(100) Fortune Nickel and Gold Inc.	21.34
613766	GOWAN	42A11	2020-10-02	2023-10-02	(100) Fortune Nickel and Gold Inc.	21.34
613767	GOWAN	42A11	2020-10-02	2023-10-02	(100) Fortune Nickel and Gold Inc.	21.34
613768	GOWAN	42A11	2020-10-02	2023-10-02	(100) Fortune Nickel and Gold Inc.	21.34
613769	GOWAN	42A11	2020-10-02	2023-10-02	(100) Fortune Nickel and Gold Inc.	21.33

613770	GOWAN	42A11	2020-10-02	2023-10-02	(100) Fortune Nickel and Gold Inc.	21.33
613771	GOWAN	42A11	2020-10-02	2023-10-02	(100) Fortune Nickel and Gold Inc.	21.34
613772	GOWAN	42A11	2020-10-02	2023-10-02	(100) Fortune Nickel and Gold Inc.	21.34
613773	GOWAN	42A11	2020-10-02	2023-10-02	(100) Fortune Nickel and Gold Inc.	21.34

*Status of the Gowan project claims are shown in the table above as of January 10th, 2023.

6. REGIONAL GEOLOGY

The Abitibi Greenstone Belt is composed of 12 distinct assemblages originating from various volcanic episodes, ranging from 2766-2677 Ma in age, as shown in Table 4 below (Thurston et al., 2008).

Table 3: Regional geological assemblages of the Abitibi Greenstone Belt.

Assemblage Name	Age (Ma)	Dominant Rock Types
Timiskaming	2677-2670	Polymictic conglomerate and sandstone in subaerial alluvial fan, fluvial, and deltaic settings, alkaline volcanic rocks in Kirkland Lake area.
Porcupine	2690-2685	Local basal felsic pyroclastic rocks of the Krist Formation (Timmins area) overlain by turbiditic sediments (argillite to wacke).
Upper Blake River	2701-2695	Mafic to felsic volcanic units with volcaniclastic components.
Lower Blake River	2704-2701	Minor clastic metasediments overlain by high Mg and Fe tholeiites with minor tholeiitic andesite, dacite, and rhyolite forming upper 5%.
Upper Tisdale	2706-2704	Intermediate to felsic amygdaloidal flows heterolithic debris flows, and volcaniclastic units.
Lower Tisdale	2710-2706	Mafic volcanic rocks with localized ultramafic, intermediate to felsic volcanics and iron formation.
Upper Kidd-Munro	2717-2711	Mafic volcanic rocks with localized ultramafic and felsic volcanics and graphitic metasediments.
Lower Kidd-Munro	2719-2717	Intermediate-felsic calc-alkaline rocks.
Stoughton-Roquemaure	2723-2720	Tholeiitic basalts with komatiites and local felsic volcanic rocks.
Deloro	2734-2724	Mafic to felsic calc-alkaline volcanic rocks with local tholeiitic mafic volcanic units and an iron formation cap.
Pacaud	2750-2735	Ultramafic, mafic, and felsic volcanic, with minor iron formation.

Volcanogenic massive sulphide (VMS) deposits have yielded about 700 million tons of copper-zinc ore. The deposits are typically spatially associated with rhyolites and are most abundant within the Deloro, Kidd–Munro and Blake River assemblages. Komatiites are found in only 4 of the assemblages (Pacaud, Stoughton–Roquemaure, Kidd–Munro, and Tisdale), but only the Kidd–Munro and Tisdale host komatiite-associated nickel-copper-platinum group elements (PGE) deposits. These 2 assemblages are also distinctive in that geochemistry shows they were derived by shallower melting of the mantle plume sources than the older komatiites. Magmatic deposits have yielded about 15 million tons of nickel-copper-PGE ore in roughly equal amount from those associated with komatiites and those associated with mafic to ultramafic intrusions (Ayer et al., 2010).

Large batholiths bounding the Abitibi Greenstone Belt are variably foliated gneissic-tonalite-granodiorite intrusive complexes that structurally underlie the supracrustal rocks. These units were emplaced synchronously with volcanism and are interpreted to have been folded along with the overlying greenstone belt. The petrological diversity of these batholiths directly reflects the evolutionary development of the Abitibi Subprovince, where the distinctly bimodal crust was developed between 2750 and 2695 Ma (G.P. Beakhouse, 2011).

Metamorphism reached lower to middle greenschist grade in the Timmins area. Localized biotite may be due to potassic metasomatism associated with gold mineralization. Pressures of metamorphism of ~200 MPa measured on both sides of the Porcupine-Destor deformation zone limit the vertical offset along the deformation zone. Along the Larder Lake Cadillac deformation zone, deformation started with south-over-north thrusting-transpression on a south-dipping fault, or north-over-south movement on a north-dipping surface. Left-lateral and then right-lateral noncoaxial strain followed dip-slip movement. Ages are thus younger than those for the Porcupine-Destor deformation zone (Bateman et al., 2008).

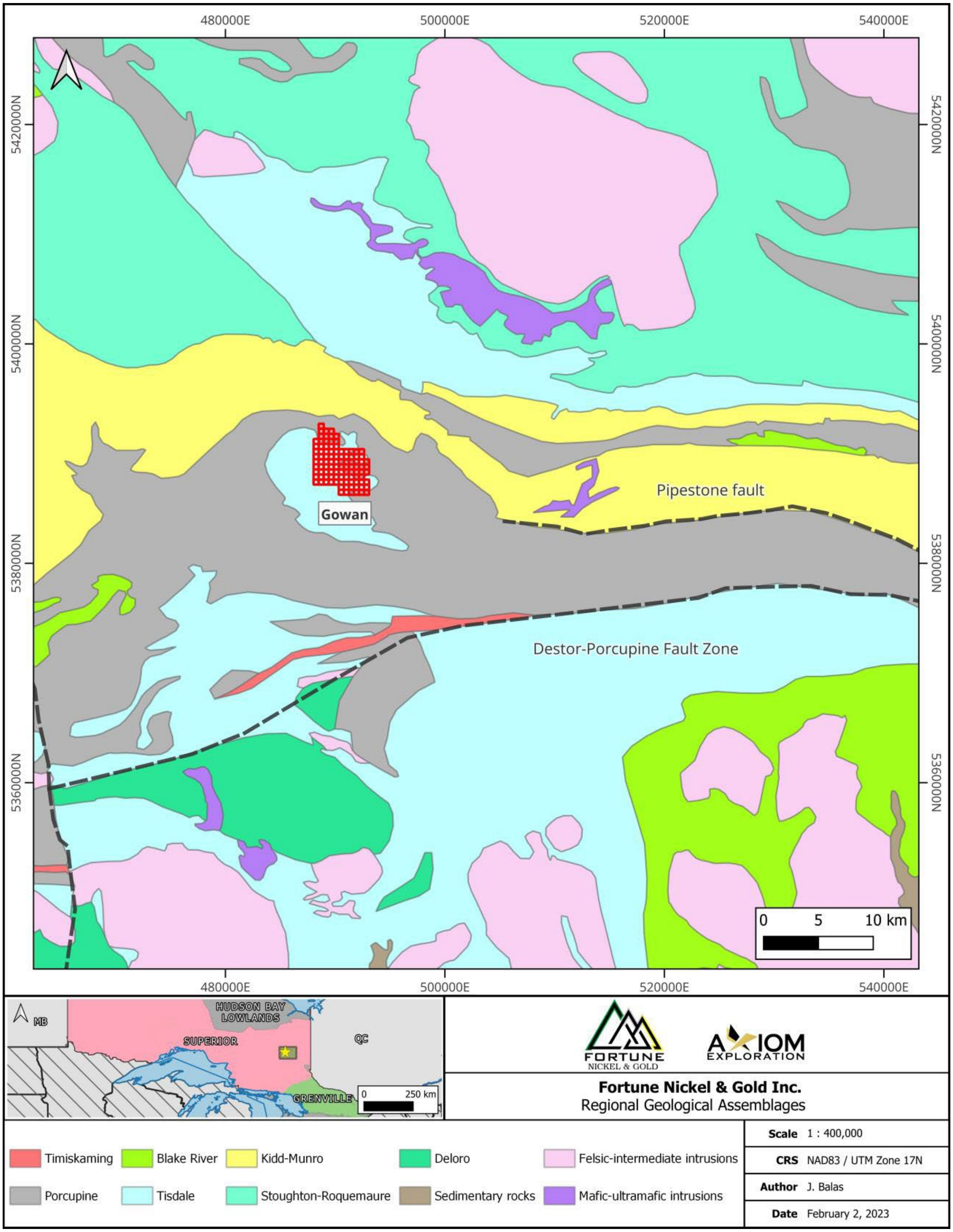

Figure 4: Regional geology surrounding the Gowan project (adapted from Pilote et al., 2019).

7. PROPERTY GEOLOGY

The Property is composed of one contiguous claim block, which is centrally located in the Gowan township and extends to encompass most of the southeast area of the township (Figure 4).

A combination of Neoarchearn ultramafic, mafic, and felsic metavolcanic rocks, metasedimentary rocks, and ultramafic and felsic intrusive rocks compose the basement of the Property. The Neoarchean basement rocks have all been affected by low grade metamorphism, as evident by porphyroblastic biotite and development of garnet in graphitic mudstone due to an ultramafic intrusion in central Gowan township, which created a thermal metamorphic halo (B.R. Berger, 1998).

The surficial geology on the Property consists of smaller sections of a variably foliated tonalite suite, which is primarily surrounded by mafic & ultramafic intrusive rocks. Ancillary sections that can also be found on the property include a granite-granodiorite complex, mafic-ultramafic metavolcanics, intermediate-mafic metavolcanics, and metasediments. Rhyolitc and dacitic dykes have been interpreted as surficial geology located immediately northeast of the Property's claim boundaries (Ontario Ministry of Mines).

The area appears to be structurally complex with little-to-no outcrops in the area due to deep clay-rich overburden. There are two parallel, northeast trending faults with unknown horizontal components that run through the property area. Perpendicular to the southern-most fault is two interpreted folds with unknown orientation (Figure 4).

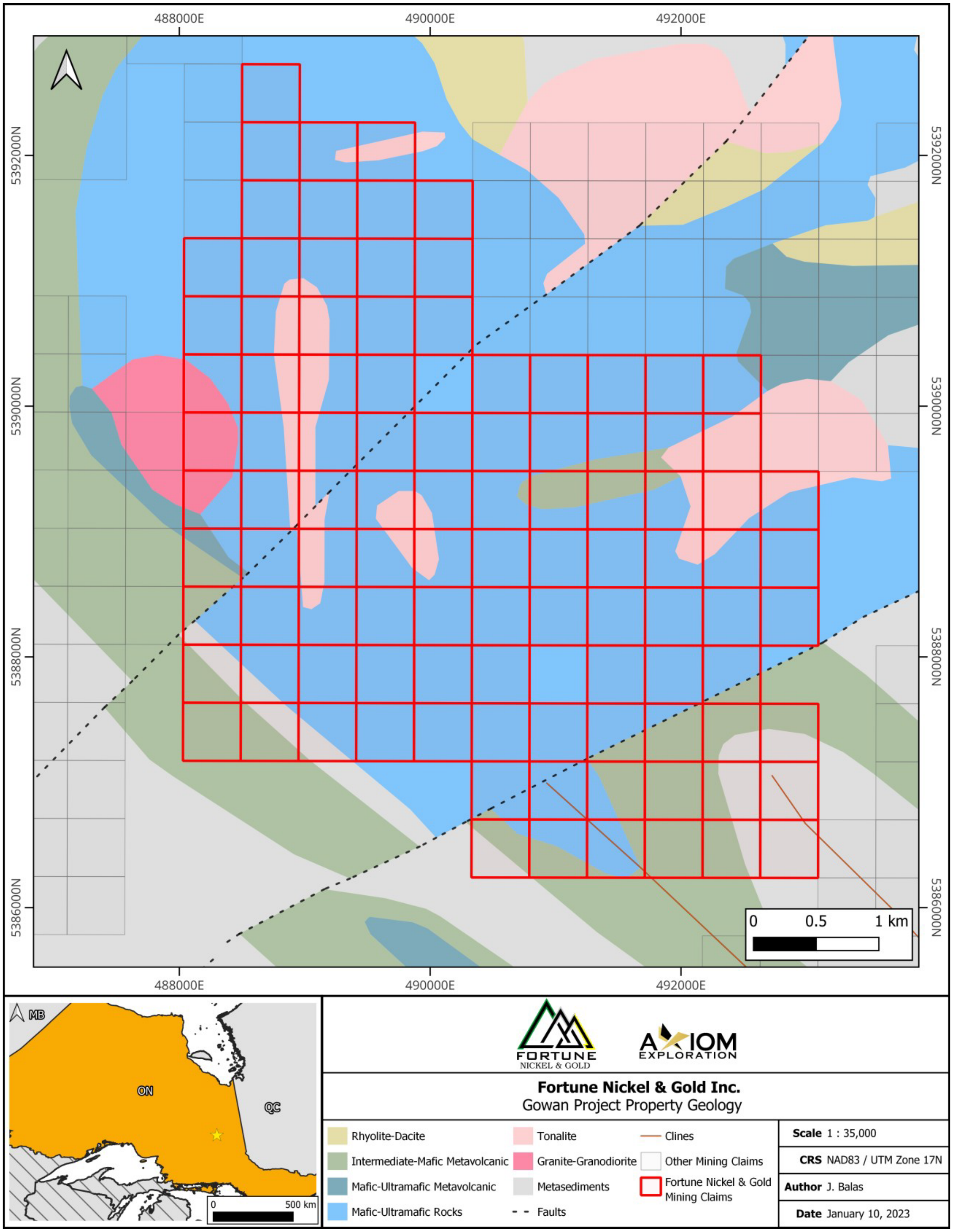

Figure 5: **Property geology of the Gowan project.**

8. Exploration History & Previous Work

The immediate Gowan project area has a long history of exploration dating back to 1960s. The following table has been adapted from the 'GeologyOntario' database and updated with recent information (Geology Ontario Database Library).

Table 4: Exploration History.

Time Period	Description of Work
1964	Airborne magnetic & electromagnetic geophysical surveys flown by Hunting Survey Corporation on behalf of Mespi Mines Ltd (R.N. Parkinson, 1964).
1965	Keevil Mining Group Limited completed two diamond drill holes in the southeastern part of the Gowan township, which encountered disseminated chalcopyrite and sphalerite (up to 2%) within graphitic mudstone at the contact with metavolcanic units of the Kidd-Munro assemblage. A syncline is inferred in this area as a combination of historical drill logs and computer-enhanced geophysical data (H.D. McLeod, 1965).
1965	Patino Mining Corporation completed two diamond drill holes int Lot 9, Concession II. Sparse specks of chalcopyrite and sphalerite were contained in units where the graphitic mudstone that was in contact with the mafic metavolcanic rocks of the Kidd-Munro assemblage (P. Eckman, 1965).
1972	Ground magnetic, induced polarization (IP), and Turam electromagnetic geophysical surveys carried out by Canex Aerial Exploration Limited. Several contacts and faults were revealed with the magnetic survey, and the electromagnetic survey identified a potential drill target (J.M. Haynes and J. Klein, 1972).
1973-1974	Reverse circulation overburden drilling was carried out by Driftex Limited on behalf of R.E. Allerston. Basal till samples returned anomalous assays of copper, nickel, and gold (S.A. Averill, 1974).
1975	Alamo Petroleum Limited optioned the property from R.E. Allerston and conducted magnetic and IP geophysical surveys to attempt to locate the overburden drilling anomalies. Subsequent diamond drilling encountered disseminated copper, silver, and zinc mineralization hosted in ultramafic rocks near the contact with felsic metavolcanic rocks. Up to 0.3% Cu and 10.6g/t was reported in one drill hole over 9.4m (R.S. Middleton, 1975a), (R.S. Middleton, 1975c), (R.S. Middleton, 1975b).
1976-1977	Newmont Exploration of Canada Limited completed ground magnetic, gradient IP and seismic geophysical surveys on the property, as well as 5 diamond drill holes which returned inconclusive results (E.J. Ballantyne, 1977a), (E.J. Ballantyne, 1977b).

1982-1984	Cominco Limited contracted Bradley Bros to conduct an extensive reverse circulation overburden drilling program, which includes over 140 reverse circulation drill holes ranging from 10 meters to 60 meters depth, and 2 diamond drill holes. This work has contributed significant data to the map relating to Quaternary and Archean geology. Assays were not reported for this drilling and the mining claims were lapsed (R.A. Gannicott, 1982), (N.L. Szabo, 1983a), (N.L. Szabo, 1983b), (N.L. Szabo, 1984).
1989-1991	Falconbridge Limited conducted an extensive exploration program over 3 years, including RC overburden drilling, magnetic and horizontal loop electromagnetic (HLEM) surveys, and four diamond drill holes were drilled to test the east extension of the favourable ultramafic contact, where some drill holes encountered spinifex textured rocks. Assay values were not reported (D.G. MacEachern, 1989), (S. Taylor, 1990), (P. Davis, 1991).
1995-1997	Geoterrex Limited flew an airborne magnetic and electromagnetic survey on behalf of Gowest Amalgamated Resources Limited. A small diamond drill program of 3 holes was completed to test geophysical targets (R.J. Bradshaw, 1995), (R.J. Bradshaw, 1997).
2018	Exsics Exploration Limited completed a moving coil pulse electromagnetic (PEM) geophysical survey on behalf of Amex Exploration Incorporated. No exploration targets were defined due to lack of penetration through thick overburden (J.C. Grant, 2018).
2020-2021	Exsics Exploration Limited completed down hole and surface Mise a la Masse IP geophysical survey on behalf of Pelangio Exploration Incorporated. The results of the survey were inconclusive in defining any mineral potential (J.C. Grant, 2021).
2021-2022	Exsics Exploration Limited completed an IP geophysical survey along 3 parallel grid lines on behalf of Fortune Nickel and Gold Incorporated. The survey outlined a conductive zone striking northeast and a potential drill target was suggested (J.C. Grant, 2022).

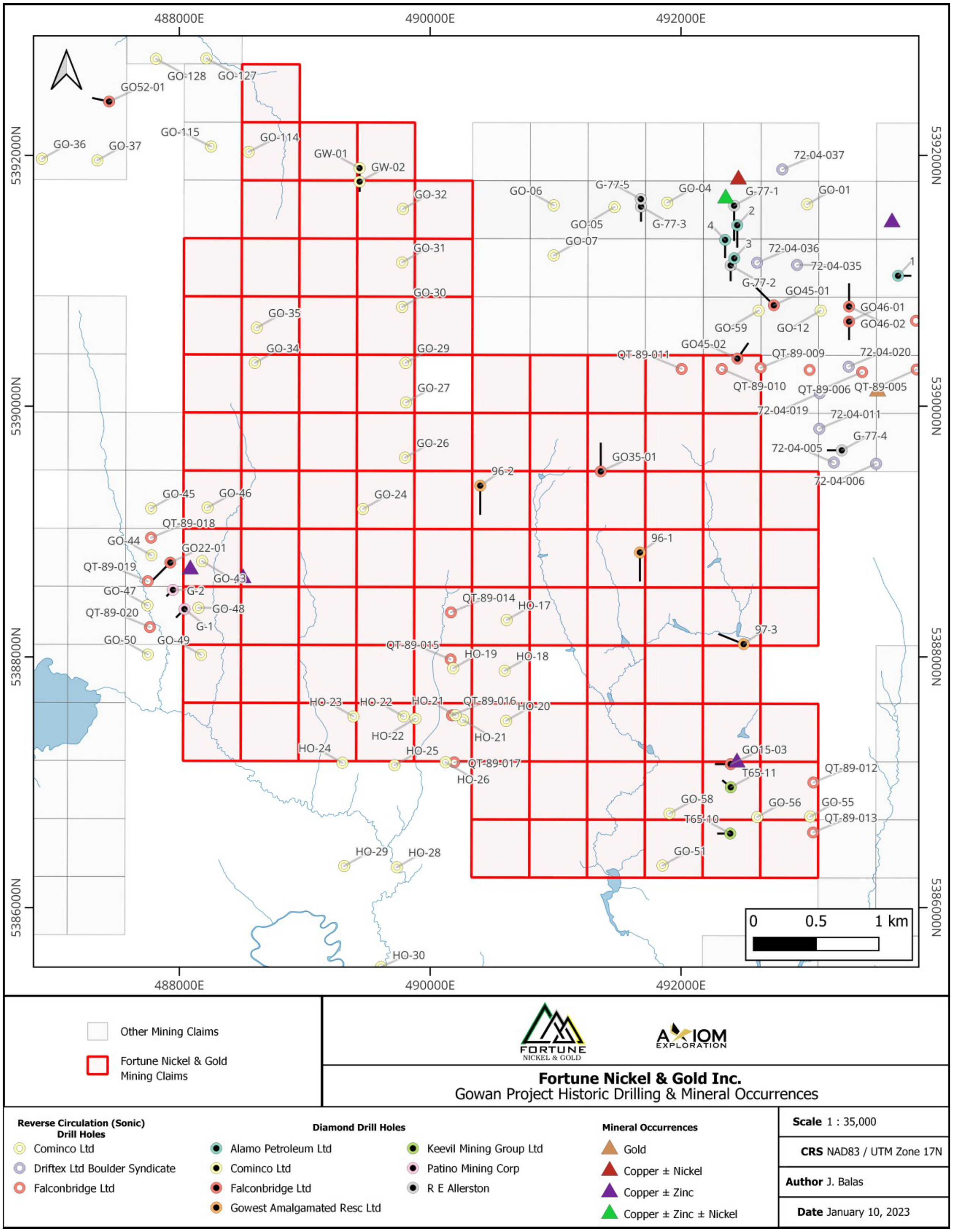

Figure 6: Historic drilling & mineral occurrences near the Gowan project area.

9. SATELLITE SENSOR TECHNICAL SPECIFICATIONS

9.1. ASTER & SENTINEL-2 (MULTISPECTRAL)

The multispectral images outlined in this report were collected from ASTER & Sentinel sensors. The images were hand picked to eliminate potential errors in analysis which may be caused by factors such as cloud cover, angle of incidence, or ground cover. The image collection dates are outlined in Table 6.

Table 5: Image collection dates for ASTER and Sentinel satellites.

Sensor	Image Collection Date
ASTER	October 7, 2000
Sentinel	May 22, 2020

The ASTER instrument on board the Terra satellite consists of three separate instrument subsystems including visible near infrared, shortwave infrared, and thermal infrared. These three subsystems include 14 spectral bands with varying resolutions as outlined in Table 7 (Satellite Imaging Corporation).

Table 6: ASTER instrument resolution characteristics (NASA).

Subsystem	Band No.	Wavelength Range (µm)	Spatial Resolution (m)	Quantization (bits)
Visible & Near Infrared (VNIR)	1	0.52-0.60	15	8
	2	0.63-0.69		
	3N	0.78-0.86		
	3B	0.78-0.86		
Short-wave Infrared (SWIR)	4	1.60-1.70	30	8
	5	2.145-2.185		
	6	2.185-2.225		
	7	2.235-2.285		
	8	2.295-2.365		
	9	2.360-2.430		
Thermal Infrared (TIR)	10	8.125-8.475	90	12
	11	8.475-8.825		
	12	8.925-9.275		
	13	10.25-10.95		
	14	10.95-11.65		

The Sentinel-2a and Sentinel-2b satellites consists of 13 spectral bands with varying resolutions as outlined in Table 8. The Sentinel-2 sensor is unique in capturing red wavelengths in three different bands, which provides key information on vegetation state (Satellite Imaging Corporation).

Table 7: Sentinel-2 instrument resolution characteristics (Delwart, 2015).

Band No.	Specific Use	Central Wavelength (µm)	Bandwidth (µm)	Spatial Resolution (m)
1	Coastal aerosol	0.443	0.020	60
2	Blue	0.490	0.065	10
3	Green	0.560	0.035	10
4	Red	0.665	0.030	10
5	Vegetation Red Edge	0.705	0.015	20
6	Vegetation Red Edge	0.740	0.015	20
7	Vegetation Red Edge	0.783	0.020	20
8	NIR	0.842	0.115	10
8b	Vegetation Red Edge	0.865	0.020	20
9	Water vapour	0.945	0.020	60
10	SWIR – Cirrus	1.375	0.030	60
11	SWIR	1.610	0.090	20
12	SWIR	2.190	0.180	20

9.2. SENTINEL-1 (SYNTHETIC APERTURE RADAR)

The SENTINEL-1 satellite carries a synthetic aperture radar instrument that operates in four acquisition modes: Stripmap (SM), Interferometric Wide swath (IW), Extra-Wide swath (EW), and Wave mode (WV). The main benefit of using synthetic aperture radar data is that it is an active sensor. SAR has the ability to capture images through cloud cover, poor illumination, and poor weather conditions. It can also capture images during the night and day, resulting in a greater variety of imagery products available (The European Space Agency).

Table 8: Sentinel-1 instrument resolution characteristics (The European Space Agency).

Mode	Incidence Angle	Resolution (m)	Swath Width (km)	Polarization (H = Horizontal; V = Vertical)
Stripmap (SM)	20-45	5 * 5	80	HH + HV, VH + VV, HH, VV
Interferometric Wide swath (IW)	29-46	5 * 20	250	HH + HV, VH + VV, HH, VV
Extra-Wide swath (EW)	19-47	20 * 40	400	HH + HV, VH + VV, HH, VV
Wave (WV)	22-35 35-38	5 * 5	20 * 20	HH, VV

10. METHODOLOGY & DATA PROCESSING

Axiom's Applied Analytics division ('AAA') utilizes proprietary in-house developed algorithms to analyze the surficial imagery data. Deep machine learning and artificial intelligence are employed whilst using multispectral imaging and synthetic aperture radar to analyze vegetation, structure, alteration, and ground movement, to effectively identify complex anomalies covering large areas. The specific case for the property resulted in maps generated for structural analysis, iron index, gossan identification, soil vegetation index ('SVI'), alunite-kaolinite-pyrophyllite abundance, hydrothermal alteration abundance, and ferric iron abundance (Figure 7, Figure 8, Figure 9, Figure 10, Figure 11, Figure 12, Figure 13).

Although AAA uses proprietary algorithms, there has been scientific research outlining the behaviour characteristics of using surficial imagery in determining geological factors, such as follows:

10.1. STRUCTURAL ANALYSIS

A structural analysis utilizes deep learning to interpretate possible structural features from geological data. The analysis uses data from satellite radar, multispectral processing, geophysics and other available maps and datasets produce the structural interpretation.

10.2. IRON INDEX

Astra satellite data is used through AAA work flows to identify areas with high iron signatures.

10.3. GOSSAN

Gossans have traditionally been identified using satellite imagery as a color combination that additionally differentiates the gossans from the alteration and the host rock. The two assemblages of minerals identified in this method are iron minerals and minerals found in hydrothermally altered rocks, which include calcite, clay, and chlorite-rich zones. In output images, red areas typically represent gossan (iron-rich) rocks, green areas represent alteration, and blue represents host (M.G. Abdelsalam and R.J. Stern, 1999).

10.4. SAVI

The Soil-Adjusted Vegetation Index (SAVI) algorithm uses a combination of NIR, Red and green vegetation cover. The output is an index between -1.0 and 1.0, which attempts to minimize soil brightness influences using a soil-brightness correction factor (Al-lami et al., 2021) (ArcGIS Pro).

The traditional SAVI equation is expressed as:

$$SAVI = ((NIR - Red)/(NIR + Red + L)) * (1 + L)$$

Where L is the amount of green vegetation cover, expressed as a ratio between 0 and 1.

This method works best in arid regions where vegetative cover is low.

10.5. Alunite-Kaolinite-Pyrophyllite Abundance

ASTER's band 6 results in lower reflectance values for OH-bearing minerals, mainly kaolinite, alunite, montmorillonite, due to an absorption feature in band 6 compared to the bands 4 and 7. Kaolinite has an additional low absorption feature in band 5, whereas alunite has absorption features in both band 5 and 8. The following band ratio reveals areas where it is likely to find alunite, kaolinite, pyrophyllite, and illite by using ASTER data for a hydrothermal alteration indicator:

Alunite-Kaolinite-Pyrophyllite indicator = (band 4 + band 6) / band 5
(Testa et al., 2018)

10.6. Hydrothermal Alteration

ASTER bands are highly sensitive to alteration minerals. Iron oxides are detected with VNIR bands. Argillic alteration is detected by band 4 of the SWIR. Propylitic alteration is detected by band 6. Phyllic alteration is detected by bands 4,5 and 8. Aluminum hydroxide minerals such as kaolinite, muscovite, montmorillonite, and illite have the highest reflection in band 4 in the SWIR, whereas magnesium hydroxide minerals such as chlorite and epidote which are indicative of propylitic alteration have the strongest reflection in band 5 and 6 in the SWIR (Bierwirth, 2002).

10.7. Ferric Iron

Rocks that are rich in ferric-iron (Fe^{3+}) typically show a sharp decline in reflectance values from approximately 0.8 µm towards shorter wavelengths. Ferric-iron rich exposures are therefore detected with ASTER 2/1 band ratio values (Salehi et al., 2019).

Additional information regarding the survey analysis can be found in Appendix A.

11. INTERPRETATION & RESULTS

Faults have been interpreted throughout the property in various locations. The main structure appears to be trending NW-SE, while a later structure cross cuts at NE-SW. A tertiary structure also appears to be trending N-S.

The relative elevation is generally decreasing from north to south. The slope appears to be gentle, ranging from approximately 268 masl from the northeast, to 244 masl in the southwest.

The iron index reflects a relatively higher iron signature from the east-central area of the Property. This region also contains intersecting faults, which could potentially be found as a correlation.

The region described above (target C from satellite maps) also displays high relative spectral signatures in all of the methods used to analyze the data, including gossan abundance, soil vegetation index, alunite-kaolinite-pyrophyllite, and hydrothermal alteration.

The resulting ferric iron abundance map from Sentinel-2 data proved to be inconclusive in finding any large anomalies. Small sections of higher spectral responses can be found scattered across the property in a non-uniform pattern.

Targets for exploration follow-up are derived from a weight of evidence approach utilizing all relevant datasets, such as DEM's, multispectral, radar, displacement, structure, alteration, specific target mineral spectra, vegetation analysis, rock discrimination analysis, false colour composites, sampling data, geological maps, weathering, soil moisture, soil mapping, and geophysics.

From a satellite perspective, bare soil and rock outcrops are not present in the Project area. Most spectral analysis therefore focussed on vegetation analysis. Certain maps, such as rock discrimination and vertical displacement maps are therefore not applicable.

Hydrothermal alteration spectral signatures that use Short Wave Infrared (SWIR) can to some extent see through vegetation. This spectral signature, together with vegetation spectral analysis and structural analysis, were the main methods that helped define the target areas.

Based on the satellite analysis, which used satellite spectra, geology, vegetation analysis, and structural analysis into account, the target areas are interpreted as associated with the major fault systems. High iron spectral values are associated with the surface fault traces and associated satellite targets.

In the Project area, vegetation is healthier (higher green signatures in spectra) over defined targets, and the positive vegetation anomalies are also associated surface fault traces, and relatively high biomass. Positive vegetation anomalies were found to be helpful in spectral target delineation.

The targets are consecutively labelled, not in prioritized order (P. Du Plessis and T. Stanley-Jones, 2023).

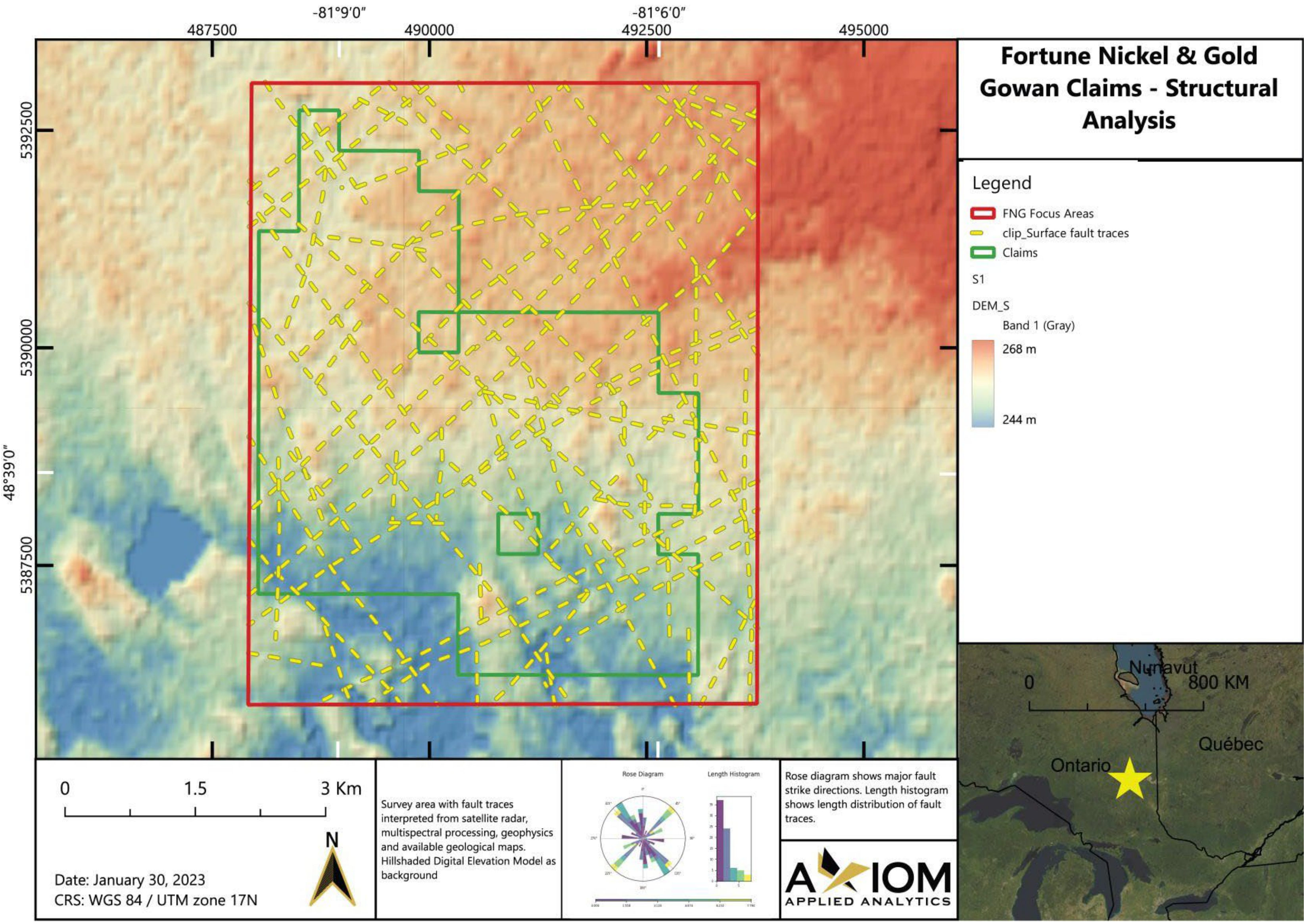

<u>Figure 7:</u> Structural analysis of the Property using ASTER satellite imagery.

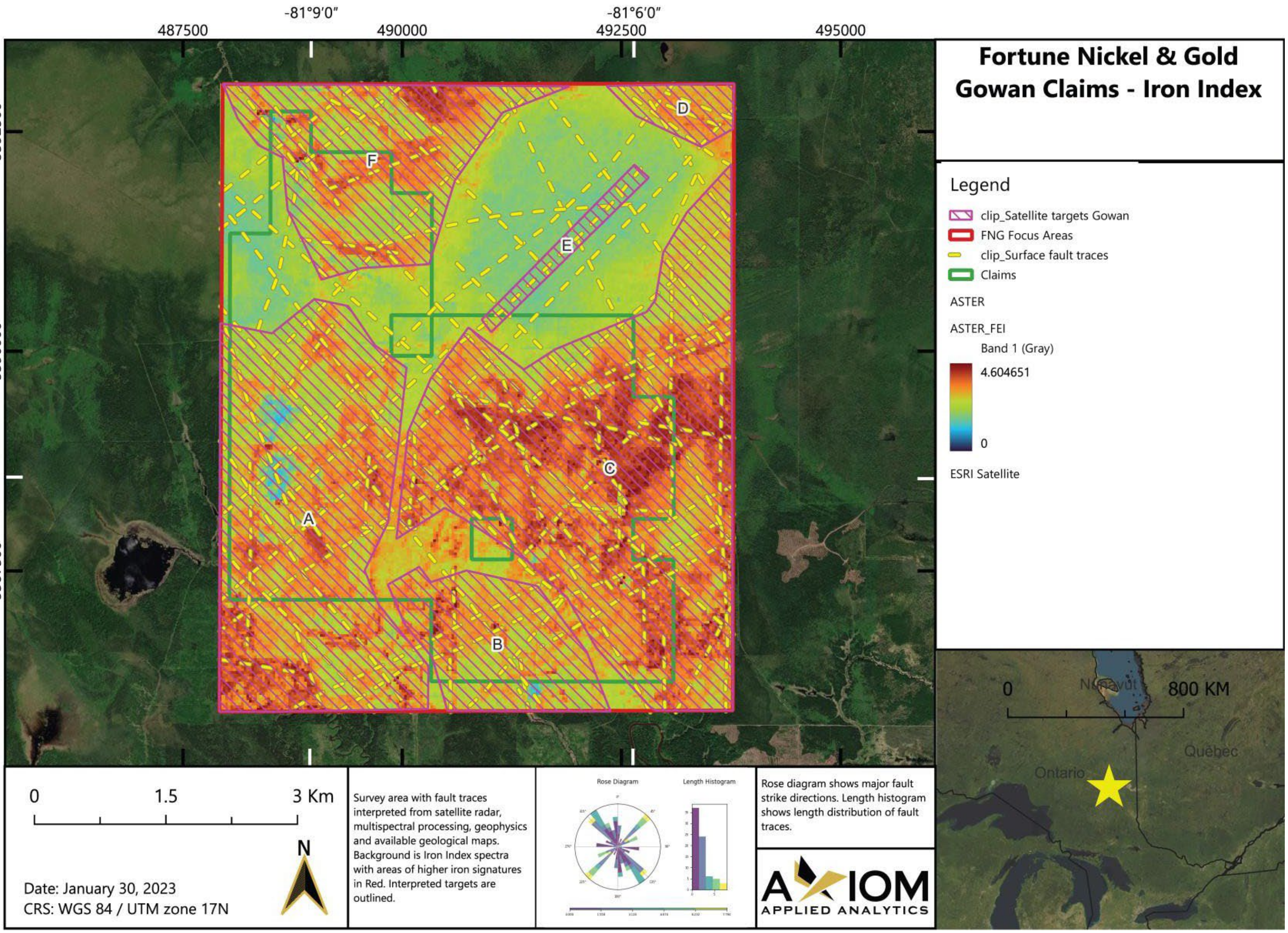

Figure 8: **Iron index of the Property using ASTER satellite imagery.**

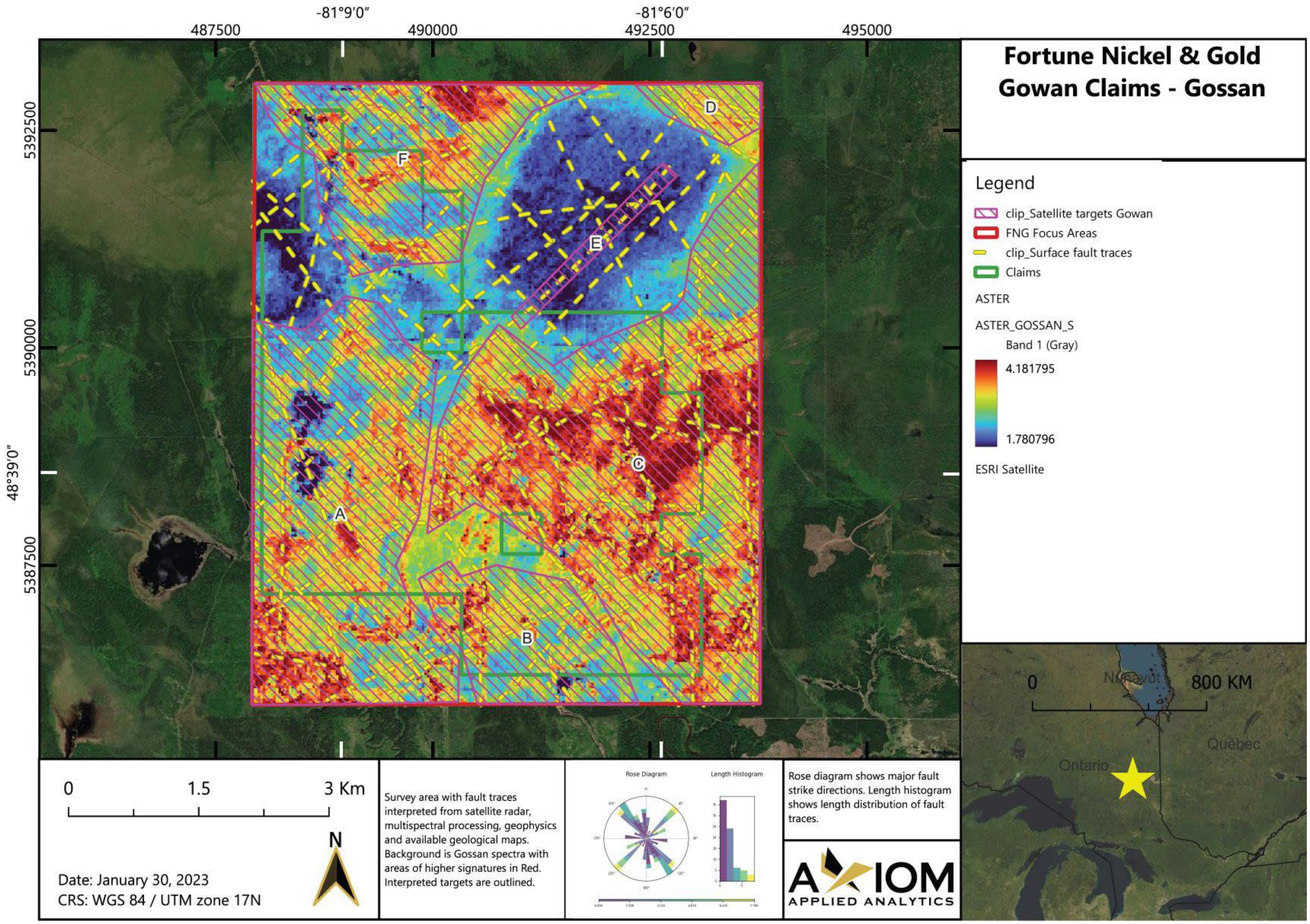

<u>Figure 9:</u> Gossan identification on the Property using ASTER satellite imagery.

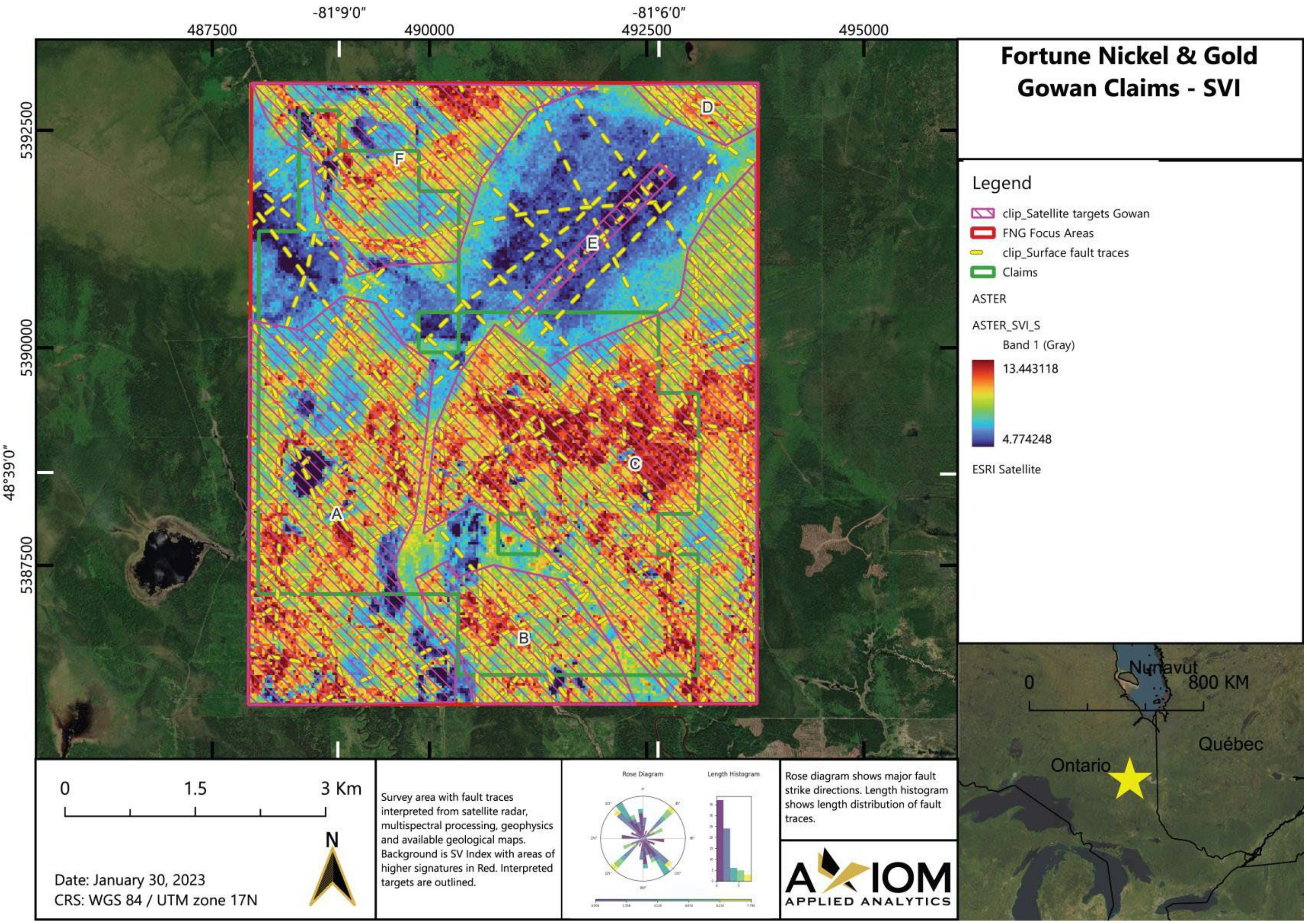

<u>Figure 10:</u> Soil vegetation index of the Property using ASTER satellite imagery.

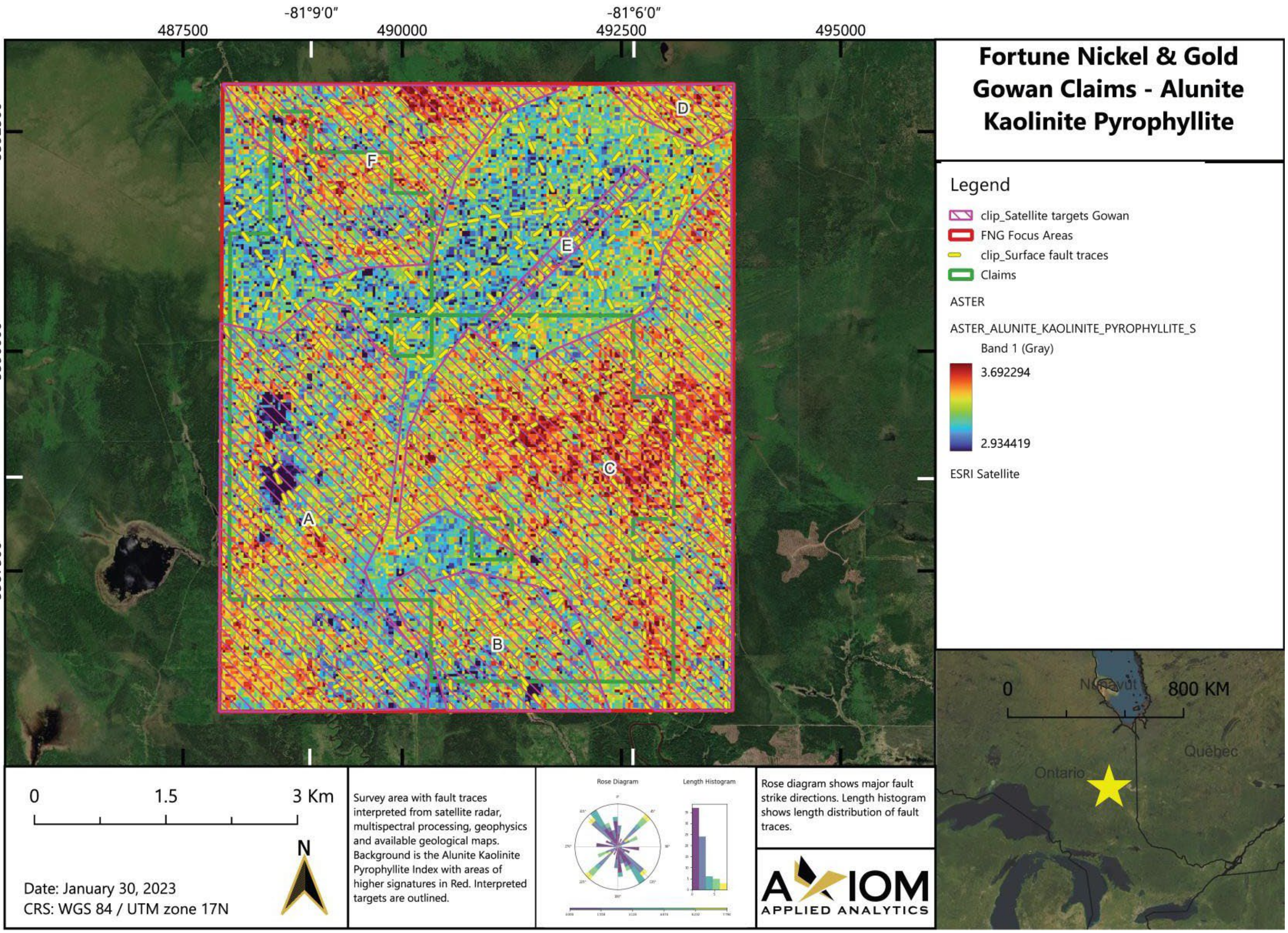

Figure 11: **Alunite-kaolinite-pyrophyllite index of the Property using ASTER satellite imagery.**

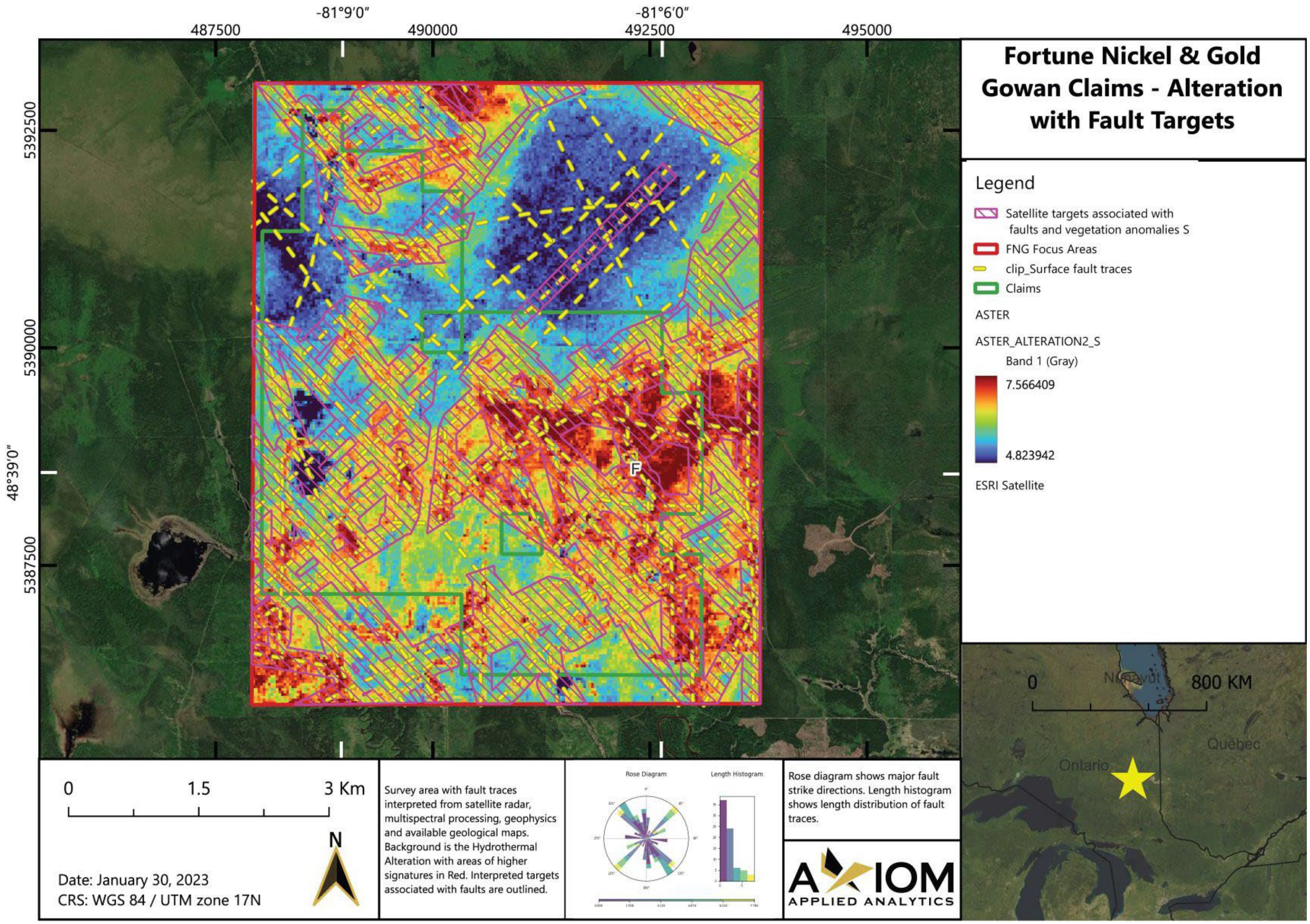

Figure 12: **Hydrothermal alteration identification of the Property using ASTER satellite imagery.**

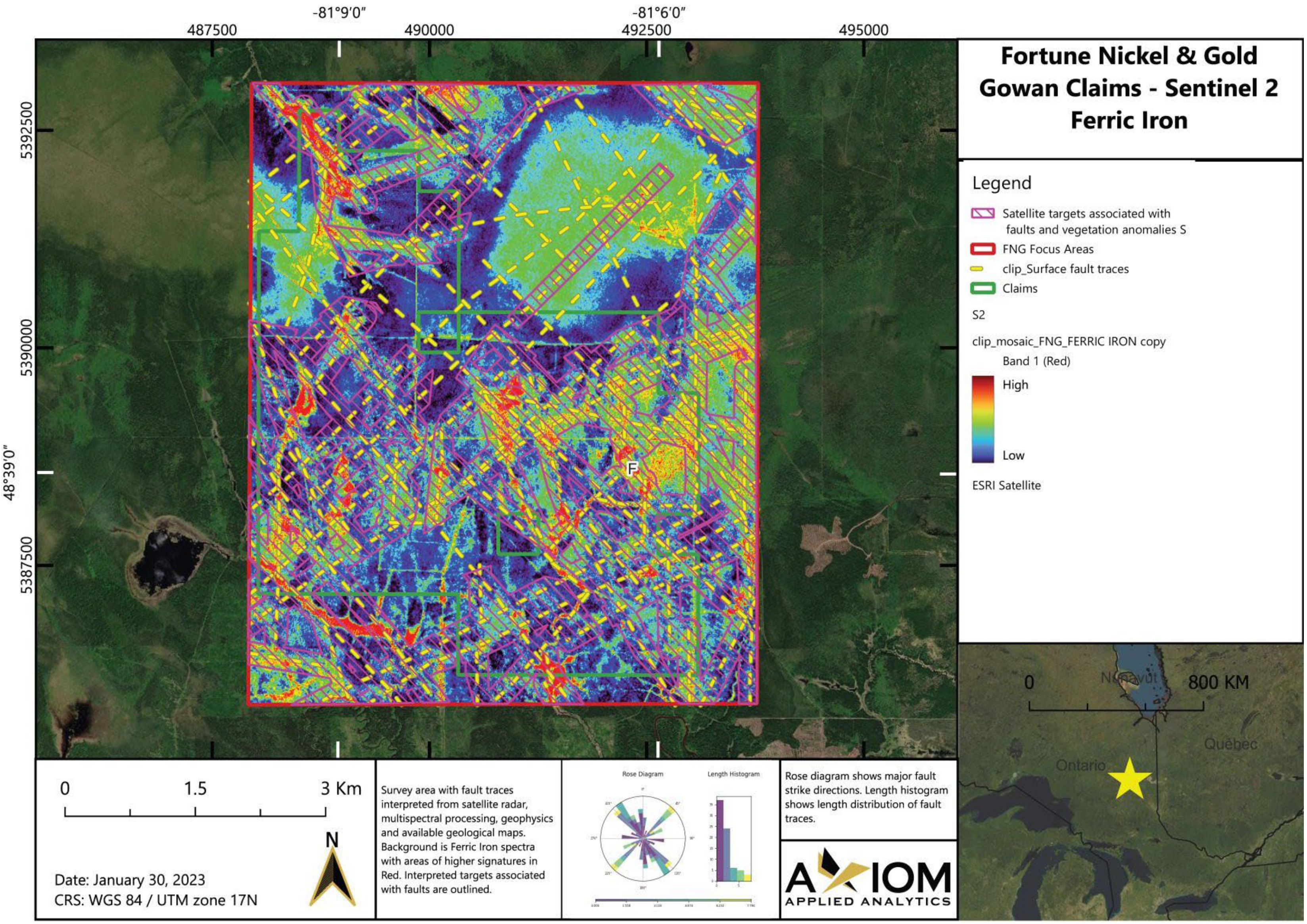

Figure 13: Ferric iron identification of the Property using Sentinel-2 satellite imagery.

12. CONCLUSIONS & RECOMMENDATIONS

The results from the re-processed satellite data were successful in generating new mineral exploration targets. However, due to the coarse spatial resolution of ASTER data within the TIR and SWIR range, the spectral signatures of surficial features contain various components within an individual pixel and may weaken or mask certain diagnostic mineral features (Salehi, Rogge et al. 2017). In other words, band ratios do not indicate the occurrence of a mineral with absolute certainty or with any idea of quantity. Therefore, it is essential to perform ground truthing and use other available data such as geological maps and geochemical and petrological datasets in conjunction with ASTER data (Salehi et al., 2019).

Recommendations for future exploration programs:

- Complete airborne TDEM geophysical survey to verify surficial exploration targets.
- Use a deep penetrating geophysical system to gain an understanding of continuity below ground surface.
- Prioritize diamond drill targets along E-W corridor through central claim package.

13. REFERENCES

Al-lami, A.K., Abbood, R.A., Al Maliki, A.A., and Al-Ansari, N., 2021, Using vegetation indices for monitoring the spread of Nile Rose plant in the Tigris River within Wasit province, Iraq: Remote Sensing Applications: Society and Environment, v. 22, p. 100471.

ArcGIS Pro, Soil Adjusted Vegetation Index (SAVI), (https://pro.arcgis.com/en/pro-app/latest/arcpy/spatial-analyst/savi.htm#:~:text=The%20Soil%2DAdjusted%20Vegetation%20Index,values%20between%20%2D1.0%20and%201.0.&text=L%E2%80%94The%20amount%20of%20green%20vegetation%20cover).

Ayer, J.A., Goutier, J., Thurston, P.C., Dubé, B., and Kamber, B.S., 2010, Tectonic and Metallogenic Evolution of the Abitibi and Wawa Subprovinces: v. 3, no. OFR 6260.

Baldwin, D.J.B., Desloges, J.R., and Band, L.E. Physical Geography of Ontario:

Bateman, R., Ayer, J.A., and Dube, B., 2008, The Timmins-Porcupine Gold Camp, Ontario: Anatomy of an Archean Greenstone Belt and Ontogeny of Gold Mineralization: Economic Geology, v. 103, no. 6, p. 1286–1287.

Beck, H.E., Zimmermann, N.E., McVicar, T.R., Vergopolan, N., Berg, A., and Wood, E.F., 2018, Present and Future Köppen-Geiger Climate Classification Maps at 1-km Resolution: Scientific Data, v. 5, no. 1, p. 180214.

Bierwirth, P.N., 2002, Evaluation of ASTER Satellite Data for Geological Applications: Consultancy Report to Geoscience Australia.

B.R. Berger, 1998, Precambrian geology, Hoyle and Gowan townships: Ontario Geological Survey Report 299.

Canadian Climate Normals 1981-2010 Station Data - Climate - Environment and Climate Change Canada, (https://climate.weather.gc.ca/climate_normals/results_1981_2010_e.html?searchType=stnName&txtStationName=Timmins&searchMethod=contains&txtCentralLatMin=0&txtCentralLatSec=0&txtCentralLongMin=0&txtCentralLongSec=0&stnID=4180&dispBack=1).

Cook, F.A., Percival, J.A., and Clowes, R.M. Tectonic Styles in Canada: Lithoprobe Perspectives on the Evolution of the North American Continent: v. Chapter 8.

Crins, W.J., 2009, Ecosystems of Ontario. Part 1, Ecozones and ecoregions: Toronto, Ont., Ontario, Ministry of Natural Resources, Inventory, Monitoring and Assessement Section.

D. Londry, 1996, Report on Geophysical Work, Gowan Property:, 3–5 p.

Delwart, S., 2015, Sentinel-2 User Handbook: European Space Agency, no. 1.

D.G. MacEachern, 1989, Reverse Circulation Overburden Drilling Report for Assessment, Gowan Township: Falconbridge Limited 42A11NE8380, 42A11NE0504, 42A11NE0505, 42A11NE0506.

Ecoregions Working Group, 1989, Ecoclimatic Regions of Canada, First Approximation: Sustainable Development Branch, Canadian Wildlife Service, Environment Canada.

E.J. Ballantyne, 1977a, Gowan Project Report: Newmont Exploration of Canada Limited 42A11NE0804.

E.J. Ballantyne, 1977b, Report of Magnetic Survey on Mining Claims in Gowan Township, Ontario: Newmont Exploration of Canada Limited 42A11NE0518.

Geo-Environmental Site Report, Gowan Mining Claims, 2020, Prairie Fire Enterprises Incorporated.

Geology Ontario Database Library, (https://www.geologyontario.mndm.gov.on.ca/index.html).

G.P. Beakhouse, 2011, The Abitibi Subprovince Plutonic Record: Tectonic and Metallogenic Implications: Ontario Geological Survey, v. Open File Report, no. 6268, p. 32–33.

H.D. McLeod, 1965, Diamond Drilling Report on Gowan township.:

J.C. Grant, 2018, Geophysical Report for Amex Exploration Inc. on the Gowan Marsh Property: Amex Exploration Incorporated.

J.C. Grant, 2021, Geophysical Report for Pelangio Exploration on the Gowan Property: Pelangio Exploration.

J.C. Grant, 2022, Geophysical Report for Fortune Nickel and Gold Inc. on the Gowan Property: Fortune Nickel and Gold Incorporated.

J.M. Haynes and J. Klein, 1972, Report on Ground Geophysical Surveys, Gowan Township, Timmins Area, Northern Ontario: Canex Aerial Exploration Limited.

M.G. Abdelsalam and R.J. Stern, 1999, Mineral Exploration with Satellite Remote Sensing Imagery: Examples from the Neoproterozoic Arabian-Nubian Shield: 11th International Conference of the Geological Society of Africa, Earth Resources for Africa.

NASA, ASTER Instument Characteristics, Advanced Spaceborne Thermal Emission and Reflection Radiometer (https://asterweb.jpl.nasa.gov/characteristics.asp).

N.L. Szabo, 1983a, Diamond Drill Report, Gowan Property: Cominco Limited 42A11NE0510.

N.L. Szabo, 1983b, Overburden Drilling Program, Gowan Property: Cominco Limited 42A11NE0509.

N.L. Szabo, 1984, Overburden Drilling Program, Gowan Property: Cominco Limited 42A11NE0508.

Ontario Drill Hole Database, (https://www.geologyontario.mndm.gov.on.ca/ODHD_Description.html).

Ontario Ministry of Mines, Geology Ontario Bedrock Geology, (https://www.geologyontario.mndm.gov.on.ca/mndmaccess/mndm_dir.asp?type=pub&id=MRD126-REV1).

P. Davis, 1991, Diamond Drill Hole Report, Gowan Township: Falconbridge Limited 42A11NE0502.

P. Du Plessis and T. Stanley-Jones, 2023, Gowan Satellite Survey Logistics Report: Axiom Exploration Group Limited.

P. Eckman, 1965, Diamond Drilling Report on Gowan Township.:

Percival, J.A., and Easton, R.M., 2007a, Geology of the Canadian Shield in Ontario: an update: 5511, 5511 p., accessed January 17, 2023, at https://geoscan.nrcan.gc.ca/starweb/geoscan/servlet.starweb?path=geoscan/fulle.web&search1=R=223891.

Percival, J.A., and Easton, R.M., 2007b, Geology of the Canadian Shield in Ontario: An Update: 5511, 5511 p., accessed January 18, 2023, at https://geoscan.nrcan.gc.ca/starweb/geoscan/servlet.starweb?path=geoscan/fulle.web&search1=R=223891.

Pilote, J.-L., Jackson, S.E., Mercier-Langevin, P., Dubé, B., and Rhys, D., 2019, Characteristics of diagenetic and epigenetic sulphides in deformed and metamorphosed Archean carbonaceous metasedimentary rocks of the Timmins-Matheson corridor: establishing a framework for fingerprinting ore-forming processes in shear zone-hosted orogenic goldsystems: 8549, 8549 p., accessed February 3, 2023, at https://geoscan.nrcan.gc.ca/starweb/geoscan/servlet.starweb?path=geoscan/fulle.web&search1=R=313632.

R.A. Gannicott, 1982, Reverse Circulation Overburden Drilling: Cominco Limited 42A11NE0513.

R.J. Bradshaw, 1995, Geological Interpretation of the Airborne Magnetic & Geotem Electromagnetic Multicoil Survey (Geoterrex): Gowest Amalgamated Resources Limited 42A11NE0084.

R.J. Bradshaw, 1997, Diamond Drill Record, Gowan Township.:

R.N. Parkinson, 1964, Report on the Conduct of an Airborne Geophysical Survey in the District of Cochrane.:

R.S. Middleton, 1975a, Induced Polarization - Resistivity Survey, East Claim Group, Gowan Township, Ontario: Alamo Petroleum Limited 42A11NE0519.

R.S. Middleton, 1975b, Summary Report on Initial Diamond Drilling Program, Gowan Township, Ontario: Alamo Petroleum Limited 42A11NE0526.

R.S. Middleton, 1975c, Vertical Loop Ground Electromagnetic Survey, West Claim Group, Gowan Township, Ontario: Alamo Petroleum Limited 42A11NE0524.

S. Taylor, 1990, Report on Geophysical Work on Gowan Grid 1, Gowan Township: Falconbridge Limited 42A11NE0501.

S.A. Averill, 1974, Overburden Drilling Report on the R.E. Allerston Option, Gowan Township, Ontario: Driftex Limited 42A11NE0521.

Salehi, S., Símun D Olsen, Pedersen, C.B., and Thorning, L., 2019, ASTER data analysis applied to mineral and geological mapping in North East Greenland Documentation of the NEG ASTER Project:

Satellite Imaging Corporation, ASTER Satellite Sensor, (https://www.satimagingcorp.com/satellite-sensors/other-satellite-sensors/aster/).

Satellite Imaging Corporation, Sentinel-2A Satellite Sensor, (https://www.satimagingcorp.com/satellite-sensors/other-satellite-sensors/sentinel-2a/).

Skinner, R.G., 1973a, A millerite occurrence in Overburden northeast of Timmins, Ontario: Terrain Sciences Division Project 710080 73–1B, 213–214 p., accessed January 12, 2023, at https://geoscan.nrcan.gc.ca/starweb/geoscan/servlet.starweb?path=geoscan/fulle.web&search1=R=104934.

Skinner, R.G., 1973b, A Millerite Occurrence in Overburden Northeast of Timmins, Ontario: 73–1B, 73–1B p., accessed January 18, 2023, at https://geoscan.nrcan.gc.ca/starweb/geoscan/servlet.starweb?path=geoscan/fulle.web&search1=R=104934.

Testa, F., Villanueva, C., Cooke, D., and Zhang, L., 2018, Lithological and Hydrothermal Alteration Mapping of Epithermal, Porphyry and Tourmaline Breccia Districts in the Argentine Andes Using ASTER Imagery: Remote Sensing, v. 10, no. 2, p. 203.

The European Space Agency, Sentinel-1: Overview, (https://sentinel.esa.int/web/sentinel/missions/sentinel-1/overview).

The European Space Agency, Sentinel-1: Resolution and Swath, (https://sentinel.esa.int/web/sentinel/missions/sentinel-1/instrument-payload/resolution-swath).

Thurston, P.C., Ayer, J.A., Goutier, J., and Hamilton, M.A., 2008, Depositional Gaps in Abitibi Greenstone Belt Stratigraphy: A Key to Exploration for Syngenetic Mineralization: Economic Geology, v. 103, no. 6, p. 1097–1134.

T.P. Gemmel, 2013, Geology of the Kidd Creek Deep Orebodies - Mine D:

Wester, M.C., Henson, B.L., Crins, W.J., Uhlig, P.W.C., and Gray, P.A. The Ecosystems of Ontario: Part 2: Ecodistricts:

Wester, M.C., Henson, B.L., Crins, W.J., Uhlig, P.W.C., and Gray, P.A. The Ecosystems of Ontario: Part 2: Ecodistricts:

14. NOTES & OTHER RELEVANT INFORMATION

All UTM coordinates included in this report were measured in NAD83 (Zone 17N), and all elevations are referenced from ‘meters above mean sea level’.

No additional information or explanation is necessary to make this assessment report understandable and not misleading.

APPENDIX A: AXIOM APPLIED ANALYTICS LOGISTICS REPORT & DELIVERABLES

AXIOM GROUP

AXIOM EXPLORATION GROUP LTD.
SUITE 101 - 3239 FAITHFULL AVENUE
SASKATOON, SK, CANADA

SATELLITE DATA ACQUISITION & ANALYSIS OVER THE GOWAN PROJECT

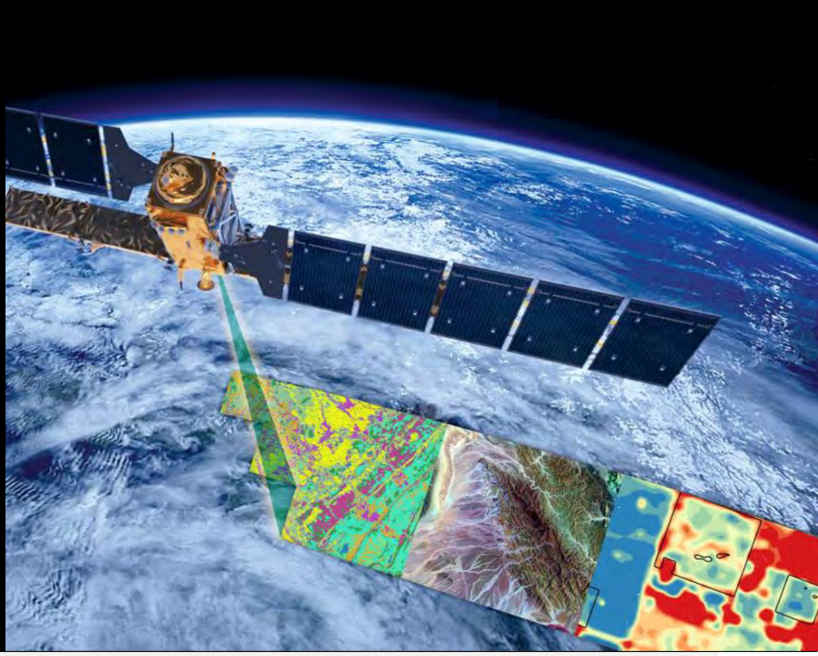

PROJECT #: 2223.7106.FNG

January 30, 2023
PIEER DU PLESSIS
THOMAS STANLEY-JONES

PREPARED FOR:
Fortune Nickel & Gold
800 Westchester
Ry Brook, NY, USA
10573

Table of Contents

LIST OF FIGURES

LIST OF TABLES

1. Executive Summary

Fortune Nickel & Gold ('the Client') engaged the services of Axiom Exploration Group Ltd. for the acquisition, processing, and analysis of synthetic aperture radar data and multispectral Sentinel, and Aster data over their project area in Ontario, Canada.

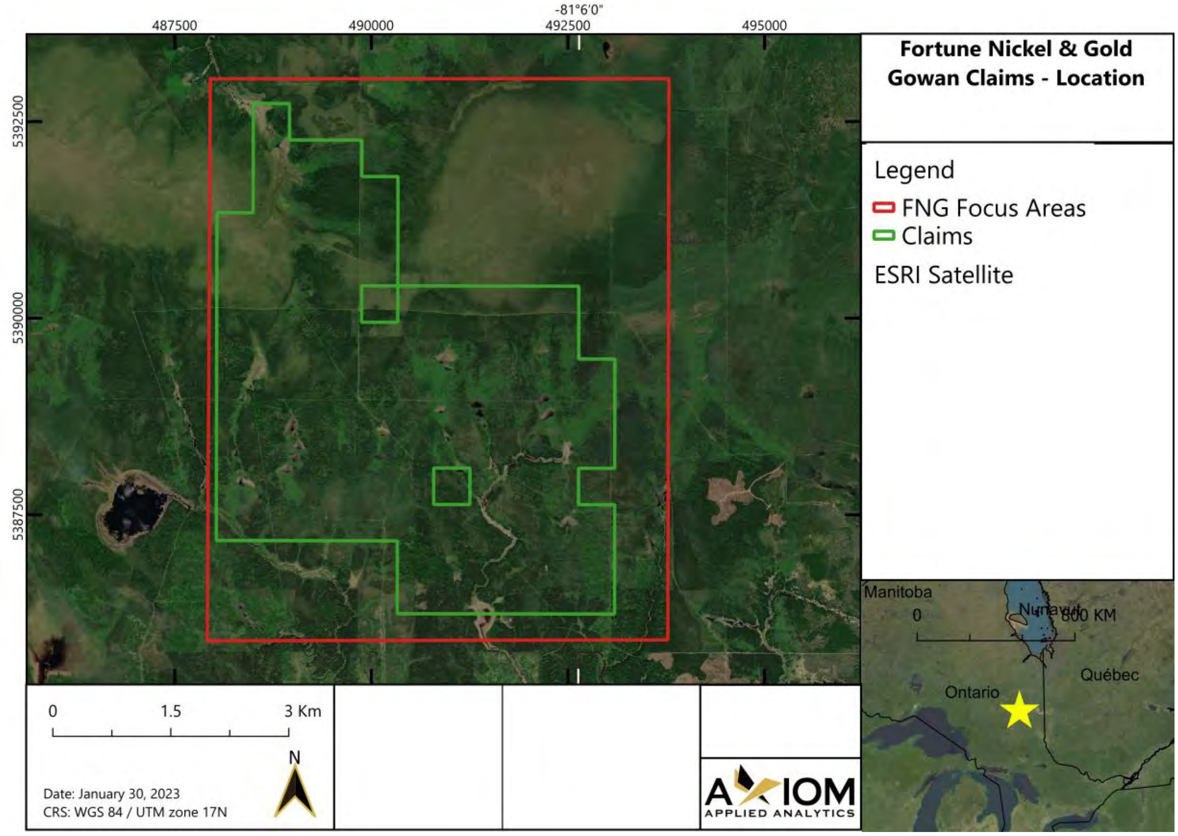

FIGURE 1: SURVEY LOCATION

The total area surveyed covers approximately 40 Km^2. This work included:

- Acquisition of the available satellite synthetic aperture radar data over property area
    - Processing, analyzing, and providing interpretation of all data collected
- Providing the Client with a DEM in their preferred format
- Collection of multispectral Sentinel & Aster data over both property areas
    - Processing, analyzing, and interpretation of multispectral data
- Reporting and analysis of all multispectral data

TABLE 1: SATELLITE SURVEY PARAMETERS

SURVEY AREA	SURVEY SIZE (KM²)	DATA TYPES TO BE ACQUIRED
Gowan Project	40	Synthetic Aperture Radar & Multispectral Data

2. Survey Details

2.1. Methodologies

By combining modern remote sensing techniques using multispectral imaging and synthetic aperture radar to analyze vegetation, structure, alteration, and ground movement, complex anomalies covering large areas can be quickly and effectively identified. This is a multivariate exploration approach, combining existing geological, geochemical, and geophysical data with multiple satellite analyses, to identify new potential mineral targets. See Figures 2-7 for examples of previous target generation work using these techniques.

Vegetation Analysis

Using Sentinel 2 and ASTER multispectral data, vegetation analysis is done with proprietary algorithms employing machine and deep learning to highlight metal stressed, negative vegetation anomalies. Algorithms are also run to show positive vegetation anomalies associated with mineral anomalies. Depending on the mineralization and sediment cover, the vegetation anomalies can either be positive or negative and both are investigated in a typical satellite analysis project.

In the example below, negative vegetation satellite analyses anomalies were derived from a Lithium project in Canada, where the lithium is toxic to vegetation. (Figure 2) (10 x 10 km).

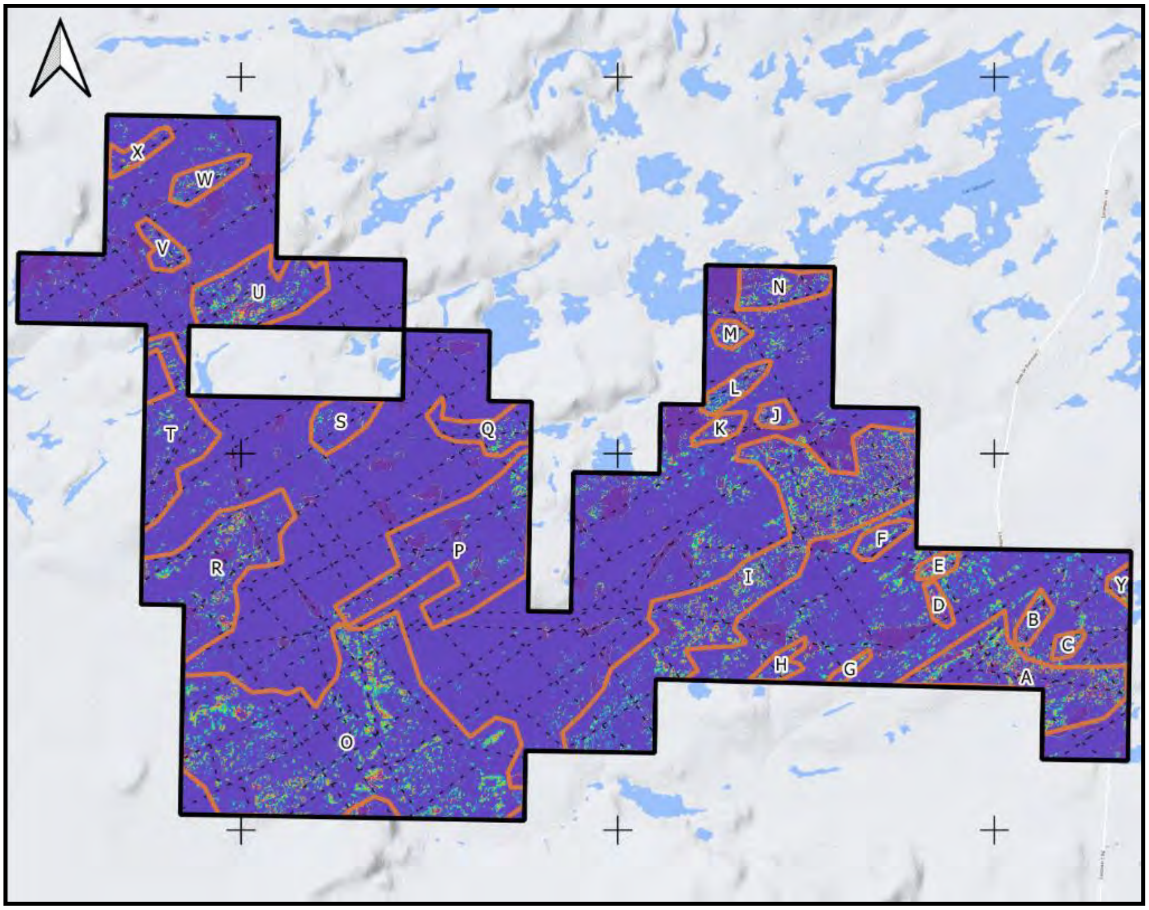

FIGURE 3: VEGETATION ANOMALIES EXAMPLE

Hydrothermal Alteration Analysis

Using machine and deep learning, Sentinel and ASTER multispectral data is analysed to highlight anomalously high hydrothermal alteration.

The high hydrothermal alteration anomalies (in warmer colours) were identified by multispectral analysis in the image below. Potential mineral exploration targets were identified by combining structural analysis (using combined multispectral analysis and radar) and the combined hydrothermal alteration anomalies.

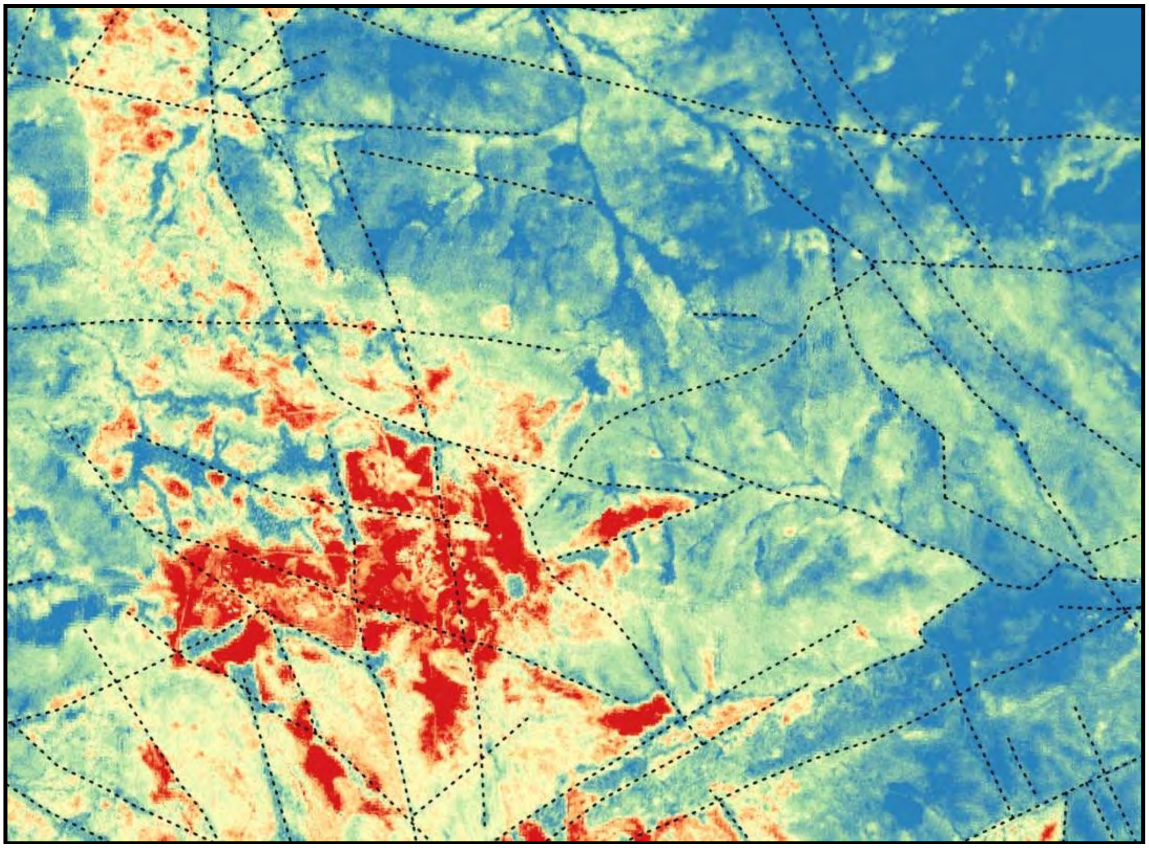

FIGURE 4: HYDROTHERMAL ALTERATION ANOMALIES EXAMPLE

We are also able to identify specific minerals from their spectral signature using satellite imagery. Figure 4 shows an example from the western United States where we identified specific mineralized clay species, including their distribution, and associated structural controls. The image on the next page illustrates the target clays in magenta and red.

Mineral Identification Analysis

By applying mineral spectral analysis to multispectral Sentinel and ASTER data, numerous minerals associated with exploration targets are identified and highlighted in georeferenced rasters. Band mathematics and statistics, utilizing the different spectral bands from multispectral satellite data, is used to isolate target minerals. The target spectra are then searched for over the whole satellite scene and anomalously high values are mapped for target delineation. Machine and deep learning are also employed on this type of data to aid in target delineation.

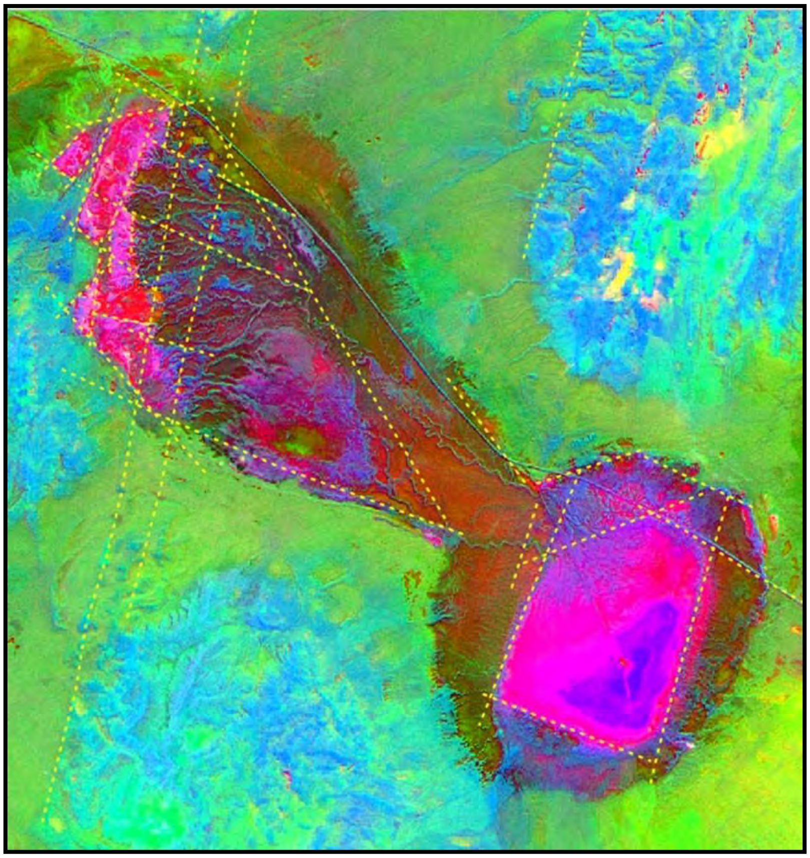

FIGURE 5: SPECIFIC MINERAL ANOMALIES IDENTIFIED FROM MULTISPECTRAL ANALYSES EXAMPLE

Subsequent field mapping and assay results confirmed the satellite mineralogical analyses, with geophysics and drilling confirming the structural analyses to a high degree of accuracy.

Using synthetic aperture radar, we can build highly accurate digital elevation models (DEMs). An example is shown in Figure 5 from a post-glacial landscape in central Canada. The area covered in this DEM is 90 km by 40 km.

Digital Elevation Model Creation

By using satellite radar interferometry DEM's can be generated at 10 m horizontal and 1 m vertical resolution, depending on the terrain. The DEM's together with satellite radar classification is used in habitat delineation and structural analysis.

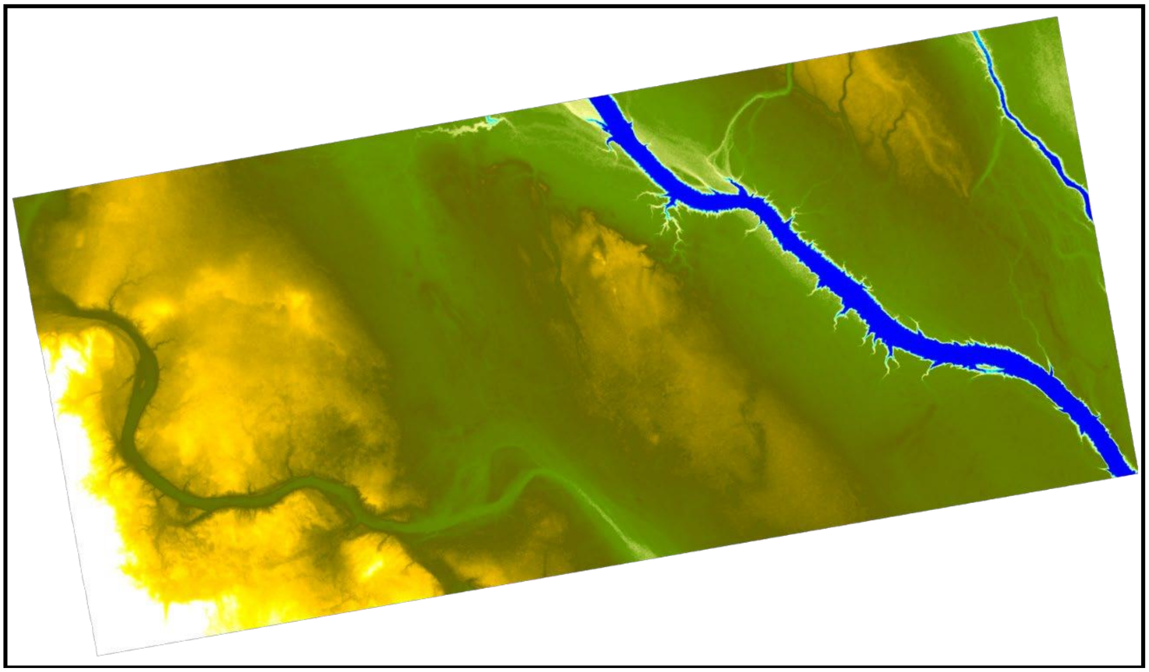

FIGURE 6: DIGITAL ELEVATION MODEL EXAMPLE

Elevation ranges from the highest in white, to the lowest in blue

Such DEM's can be used to evaluate areas for differential movement in the wet and dry seasons as clays resulting from hydrothermal alteration react differently to moisture than material from the surrounding country rock.

Using a time series of radar images one can detect active fault movements and measure displacements up to 3 mm accuracy. We can therefore detect differential swelling in clays due to moisture, subsidence, or differential tectonic movement.

The 10 x 10 km image in Figure 6 from a project in California shows major horst-graben displacement along NNW faults, parallel to the San Andreas fault line in the southwestern part of the image, measured over a one-year period to 3 mm accuracy. The displacement ranges from minus 12 cm to plus 3 cm during the one-year period.

This type of satellite analysis is used to determine the major faults and to progress the structural analysis that is crucial in understanding controls of potential mineralization. The baseline of fault movements over time is also important for mine planning activities.

Regional Structural Analysis

Utilizing satellite radar, multispectral data, any exiting geological mapping and 30 years of exploration and mining geological experience, a structural analysis is completed for exploration and mining projects to aid in the understanding of structural control on mineralization. With satellite radar vertical displacement of 3mm or more can be mapped out for the area of interest and is utilized in the structural analysis. In the vertical displacement map in Fig. 6, north-north-west striking horst and grabens can be observed in the data, actively moving vertically during the analysis period, parallel to the San Andreas fault system. Understanding the structural setting and active fault movement is key for exploration, mining and environmental applications.

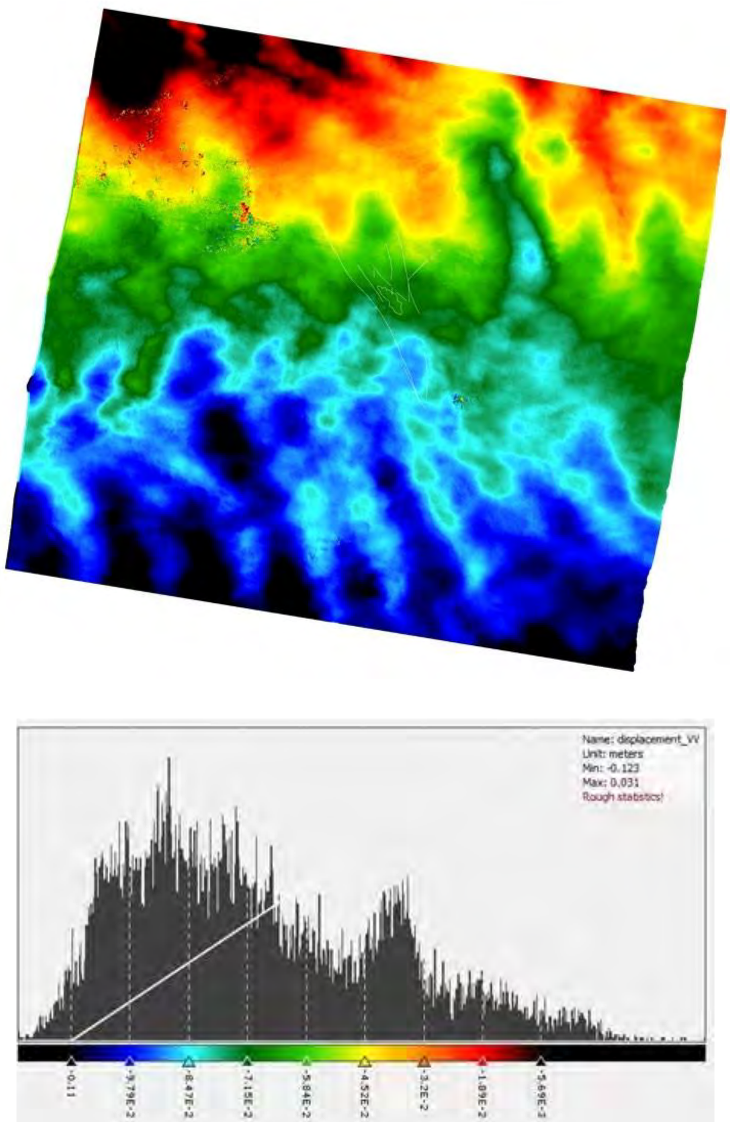

FIGURE 7: REGIONAL MOVEMENT DUE TO TECTONICS EXAMPLE

The combination of techniques outlined above, together with existing data (knowledge of known mineral occurrences, soil and stream sampling, geophysics, regional geology, etc.) can be applied to mineral exploration, using a weight of evidence approach in an area of interest to outline targets for advanced mineral exploration.

Structural Analysis & Lineament Interpretation

The example below illustrates a structural analysis performed for a client using satellite radar and multispectral data, employing 30 years of exploration, mining and terrain evaluation experience, to assist in highlighting the structural control on mineralization. The surface fault traces derived from the structural analysis is shown in purple dotted lines, draped on a hill shaded DEM background derived from satellite radar analysis. In this case study, the mineralization is controlled by the northeast striking fault system, that displaces the north-northwest striking diabase in the western part of the area of interest. A Rose diagram showing the major structural strikes typically forms part of the analysis.

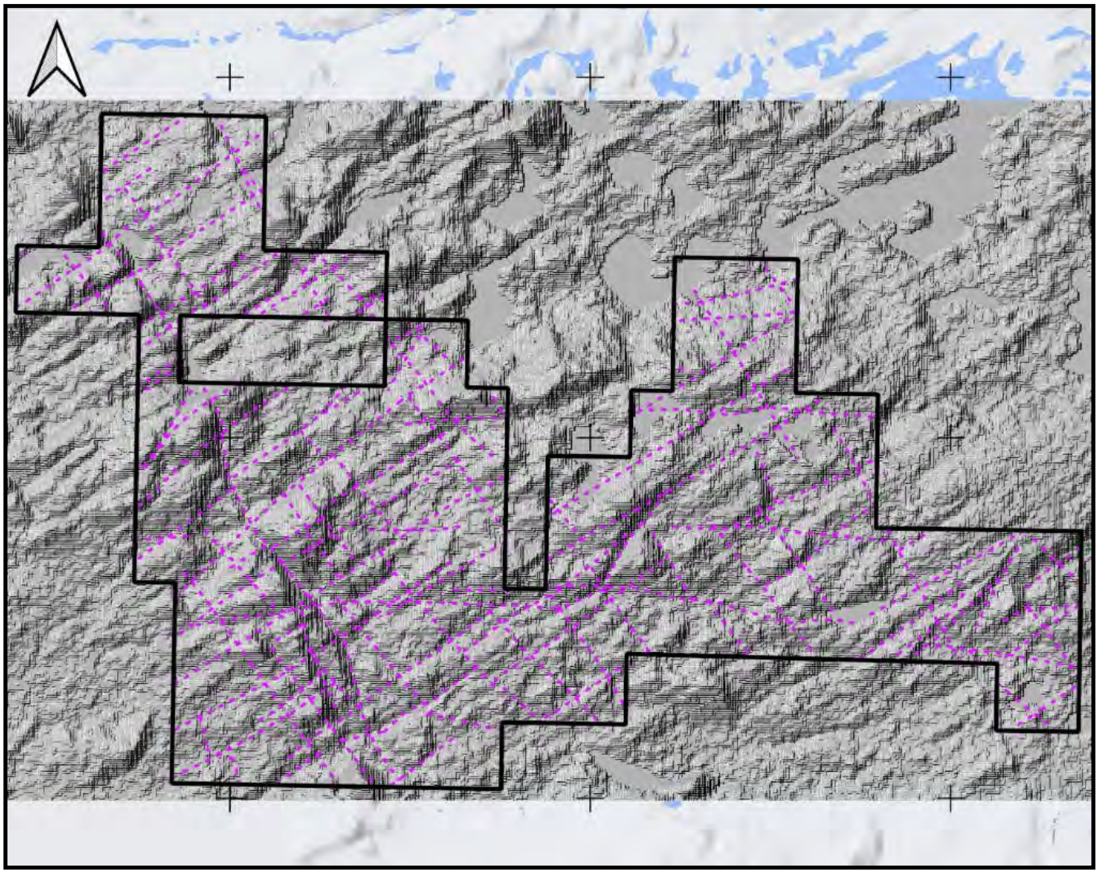

FIGURE 8: HILL SHADED DEM & STRUCTURAL INTERPRETATION EXAMPLE

The combination of satellite techniques outlined above, together with existing data (knowledge of known mineral occurrences, soil and stream samples, geophysics, regional geology, etc.) can be combined in a weight of evidence approach, using machine and deep learning to identify mineral targets. Utilizing this approach has been proven to save time and costs in exploration projects, by reducing the areas for advanced exploration work and focussing efforts and thereby improving efficiencies.

2.2. Deliverables

1. Digital elevation models (3D Topographical Models) over requested areas in client's preferred format (geotiff or others by request)
    a. 15 x 15 x 10 m resolution down to 1 m vertical resolution, depending on terrain
2. Raw Data
    a. Georeferenced Shapefiles (vector) & GEOTIFFS (raster)
3. Maps
    a. Prospectively maps - including specific exploration targets
    b. Hydrothermal alteration maps, where applicable
    c. Maps of specific alterations: argillic, phyllic, propylitic and silicic, where applicable
    d. Maps of all ferric and non-ferric oxides, where applicable
    e. Structural maps
    f. False colour composite maps
    g. Displacement maps showing active fault movement and movement over time, where applicable
    h. Rock discrimination maps where applicable
4. Report (All maps at 10 x 10 m or 30 x 30 m resolution unless otherwise stated)

Notes:

We use a multivariate approach, combining SAR with satellite multispectral soil, rock, and vegetation analysis, to detect mineralization and hydrothermal alteration spectral signatures.

The SAR is typically used by us for detecting structures and displacement to map out the regional and local structural setting, that often controls the mineralisation.

The penetration of satellite-based SAR through vegetation and soil depends on several factors:

- The density and height of vegetation, though we have used SAR successfully in the boreal forest in Canada and tropical forest in Papua New Guiney to detect structures.
- SAR can penetrate through coarse dry sand for several meters, but with increased moisture or clay content, the penetration decreases to near surface.

In limited areas of permanent ice cover DEM will provide the top-of-ice surface. Multi-year SAR data oriented from different angles, will be used to optimise the resultant DEM, and improve accuracy. The satellite radar data can see through clouds and most vegetation to detect the ground surface. Any available ground truthed elevation data will be used to refine the digital elevation models.

All products from the survey are delivered in digital form. All data is referenced to the WGS84 datum and are provided in a UTM projection unless specified otherwise.

3. Interpretation

3.1. Target Areas

Targets for exploration follow-up are derived from a weight of evidence approach utilizing all relevant datasets, such as DEM's, multispectral, radar, displacement, structure, alteration, specific target mineral spectra, vegetation analysis, rock discrimination analysis, false colour composites, sampling data, geological maps, weathering, soil moisture, soil mapping, geophysics, etc.

In evaluating all the available data, 30 years of geological, soil and plant analysis experience, with proven success in finding ore bodies using these techniques, is utilized in the process to reduce false positive anomalies.

From a satellite perspective, bare soil and rock outcrops are not present in the study area. Most spectral analysis therefore focussed on vegetation analysis. Certain maps, such as rock discrimination and vertical displacement maps are therefore not applicable.

Only a small selection of key maps are shown in the Appendix of this report. These maps, and a large number of additional georeferenced raster and vector layers from the satellite analysis, are supplied in the data package, in digital form, for easy incorporation into GIS systems.

Hydrothermal alteration spectral signatures that use Short Wave Infrared (SWIR) can to some extent see through vegetation. This spectral signature, together with vegetation spectral analysis and structural analysis, were the main methods that helped define the target areas.

Based on the satellite analysis, which used satellite spectra, geology, vegetation analysis, and structural analysis into account, the target areas are interpreted as associated with the major fault systems. High iron spectral values are associated with the surface fault traces and associated satellite targets.

In this area, vegetation is healthier (higher green signatures in spectra) over defined targets, and the positive vegetation anomalies are also associated surface fault traces, and relatively high biomass. Positive vegetation anomalies were found to be helpful in spectral target delineation.

The targets are consecutively labelled, NOT in prioritized order.

4. Appendix A: Final Maps

Fortune Nickel & Gold Gowan Claims - Structural Analysis

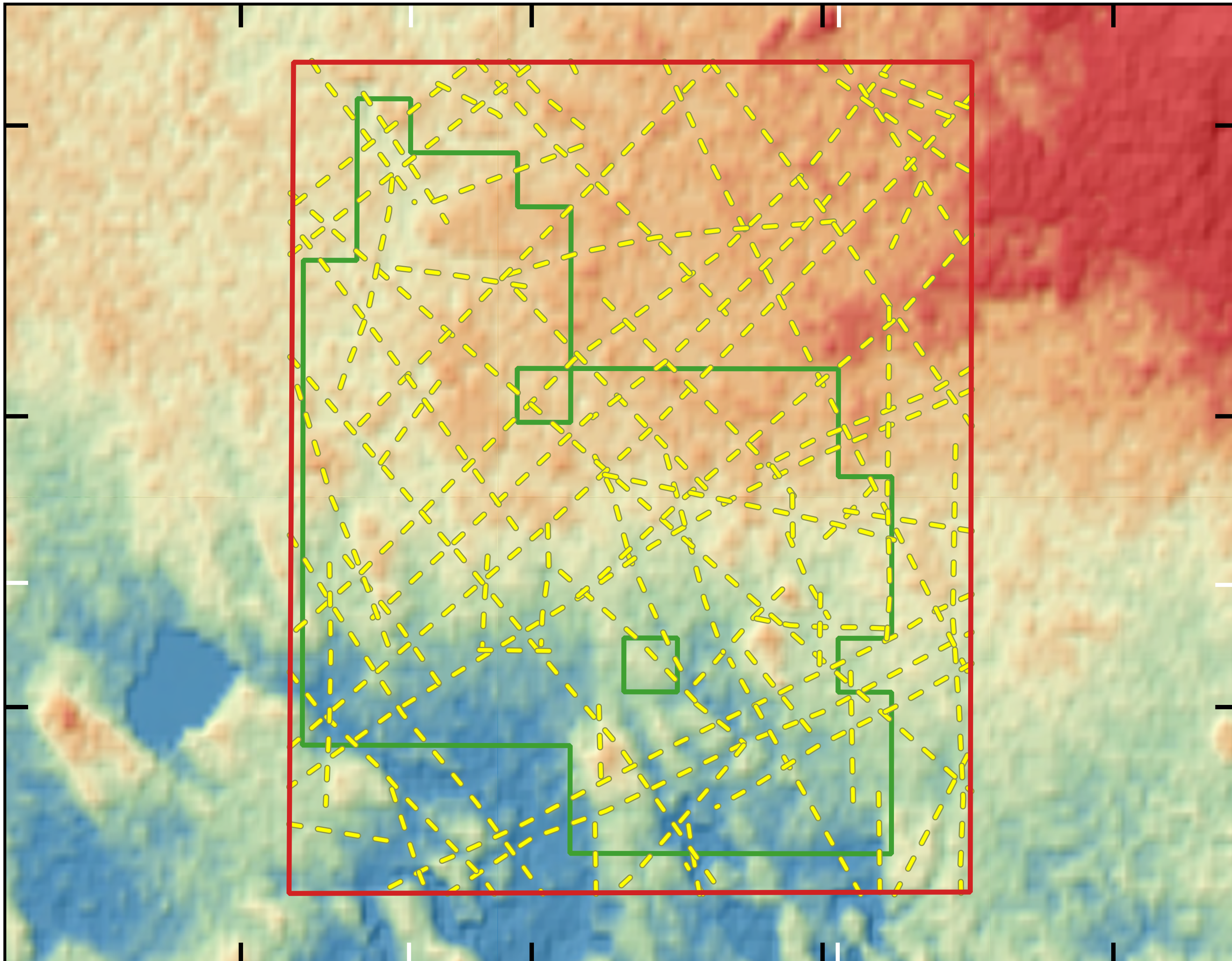

Legend

FNG Focus Areas

clip_Surface fault traces

Claims

S1

DEM_S

Band 1 (Gray)

268 m

244 m

0 1.5 3 Km

N

Date: January 30, 2023

CRS: WGS 84 / UTM zone 17N

Survey area with fault traces interpreted from satellite radar, multispectral processing, geophysics and available geological maps. Hillshaded Digital Elevation Model as background

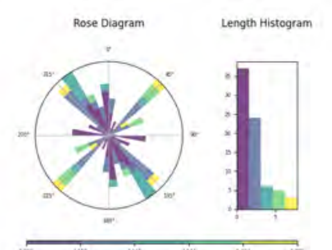

Rose diagram shows major fault strike directions. Length histogram shows length distribution of fault traces.

AXIOM APPLIED ANALYTICS

Fortune Nickel & Gold Gowan Claims - Iron Index

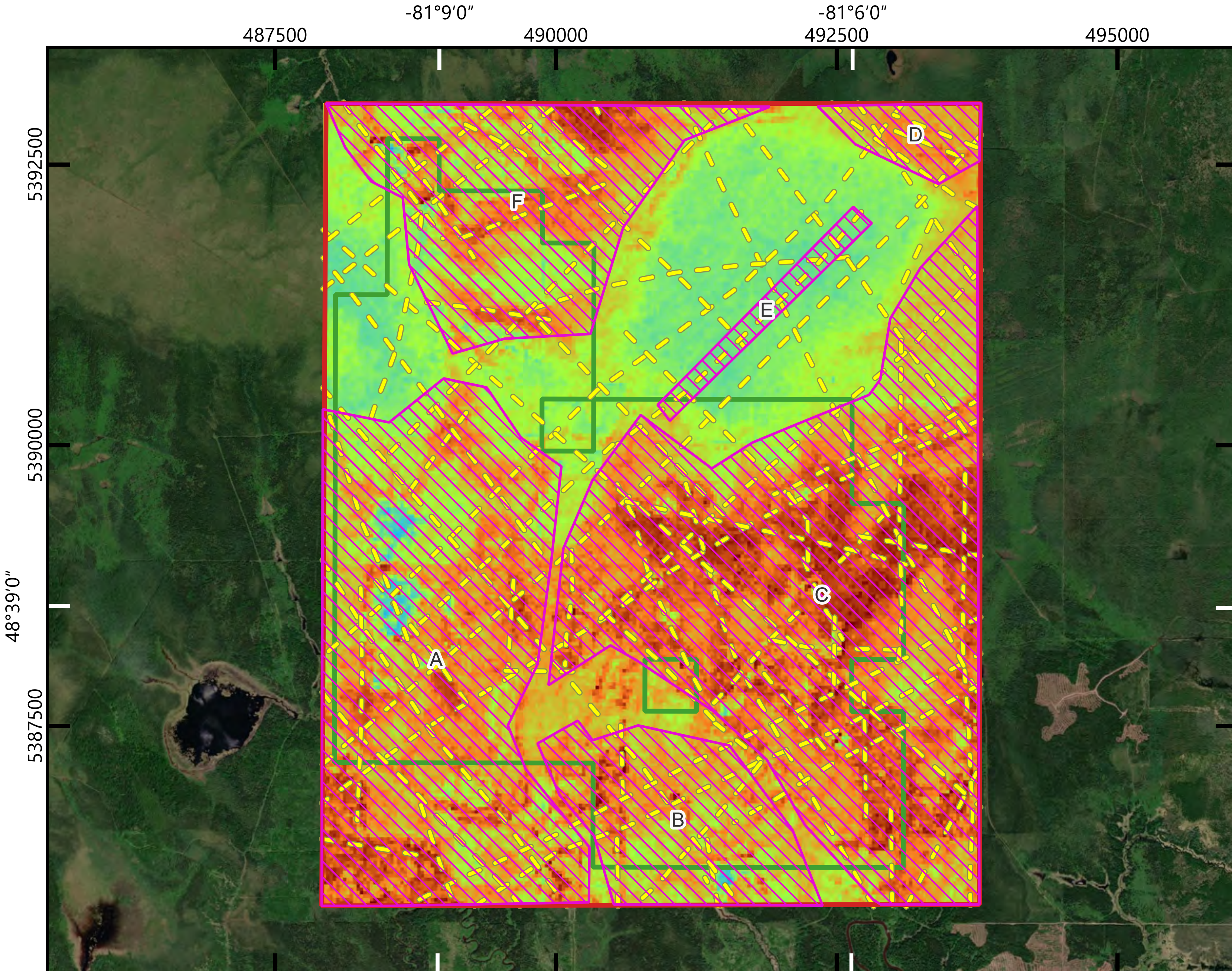

Legend

- clip_Satellite targets Gowan
- FNG Focus Areas
- clip_Surface fault traces
- Claims

ASTER

ASTER_FEI

Band 1 (Gray)

4.604651

0

ESRI Satellite

0 1.5 3 Km

N

Date: January 30, 2023

CRS: WGS 84 / UTM zone 17N

Survey area with fault traces interpreted from satellite radar, multispectral processing, geophysics and available geological maps. Background is Iron Index spectra with areas of higher iron signatures in Red. Interpreted targets are outlined.

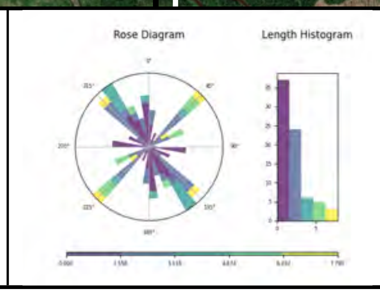

Rose diagram shows major fault strike directions. Length histogram shows length distribution of fault traces.

AXIOM APPLIED ANALYTICS

Fortune Nickel & Gold Gowan Claims - Gossan

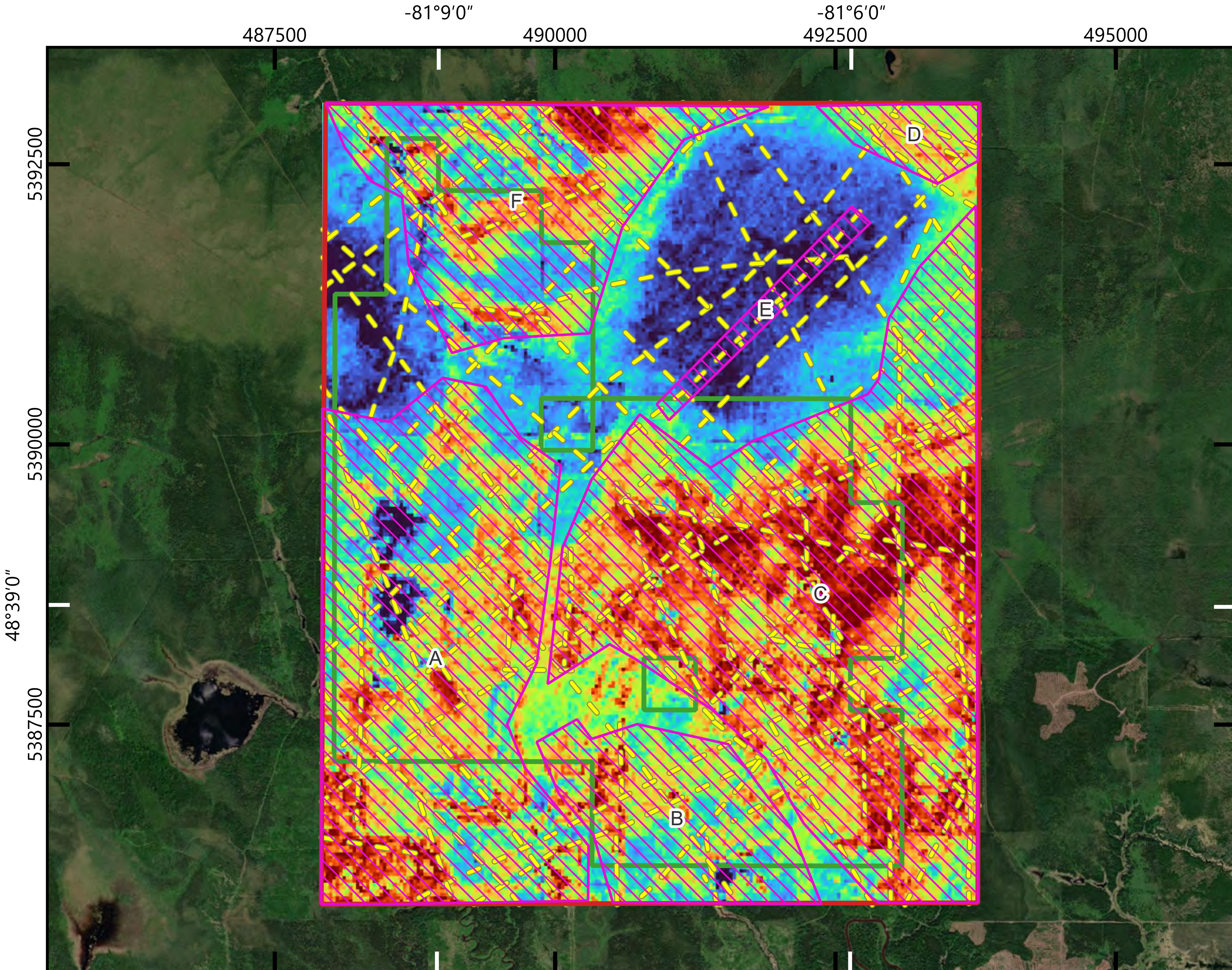

Legend

- clip_Satellite targets Gowan
- FNG Focus Areas
- clip_Surface fault traces
- Claims

ASTER

ASTER_GOSSAN_S

Band 1 (Gray)

4.181795

1.780796

ESRI Satellite

0 1.5 3 Km

N

Date: January 30, 2023

CRS: WGS 84 / UTM zone 17N

Survey area with fault traces interpreted from satellite radar, multispectral processing, geophysics and available geological maps. Background is Gossan spectra with areas of higher signatures in Red. Interpreted targets are outlined.

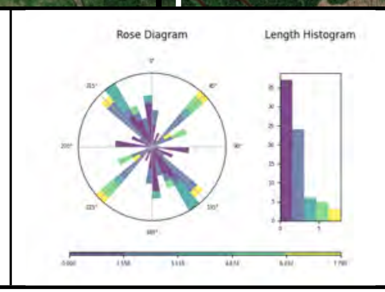

Rose diagram shows major fault strike directions. Length histogram shows length distribution of fault traces.

AXIOM APPLIED ANALYTICS

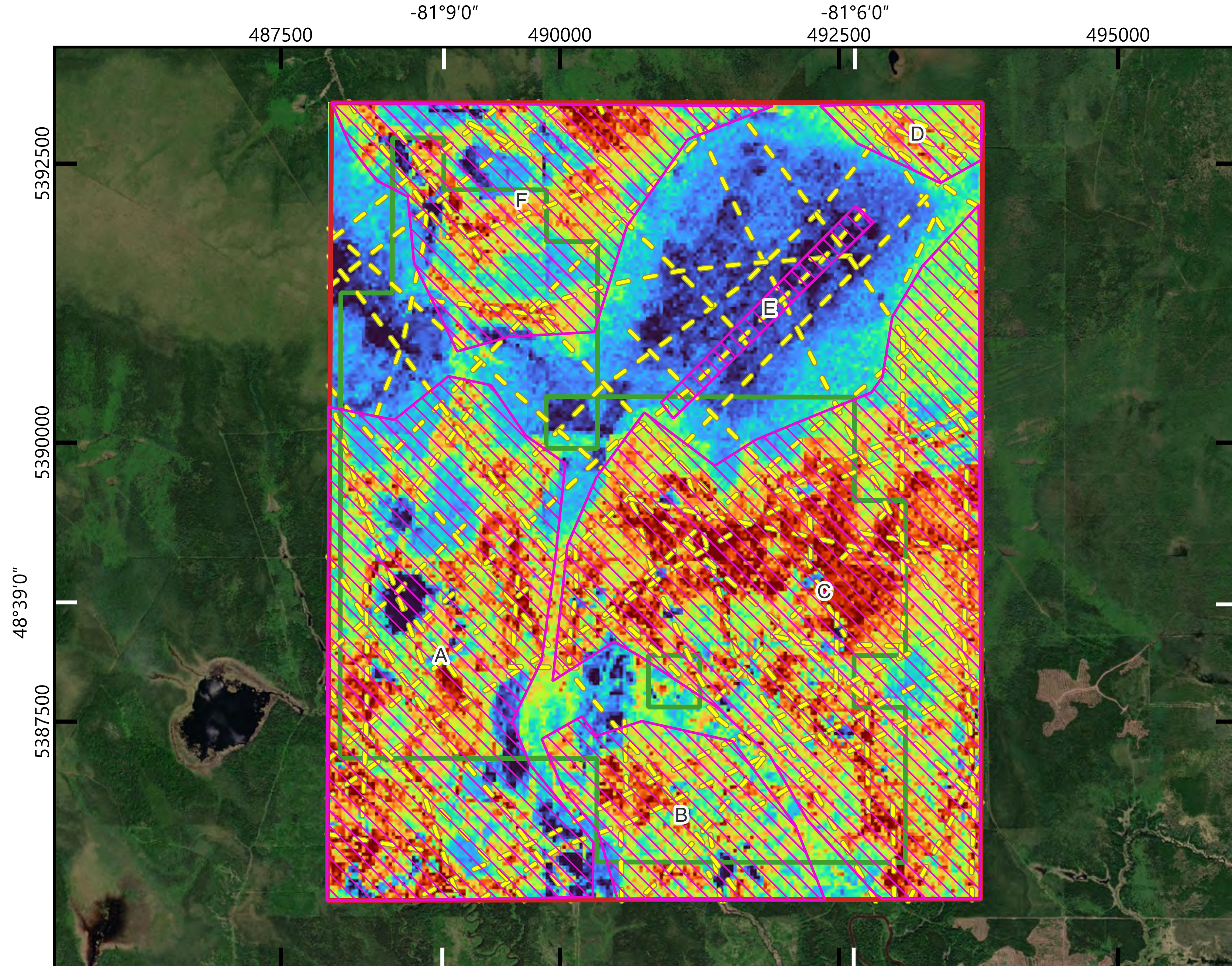

Fortune Nickel & Gold Gowan Claims - SVI

Legend

- clip_Satellite targets Gowan
- FNG Focus Areas
- clip_Surface fault traces
- Claims

ASTER

ASTER_SVI_S

Band 1 (Gray)

13.443118

4.774248

ESRI Satellite

0 1.5 3 Km

N

Date: January 30, 2023

CRS: WGS 84 / UTM zone 17N

Survey area with fault traces interpreted from satellite radar, multispectral processing, geophysics and available geological maps. Background is SV Index with areas of higher signatures in Red. Interpreted targets are outlined.

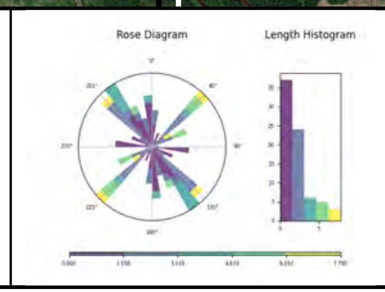

Rose diagram shows major fault strike directions. Length histogram shows length distribution of fault traces.

AXIOM APPLIED ANALYTICS

Fortune Nickel & Gold Gowan Claims - Alunite Kaolinite Pyrophyllite

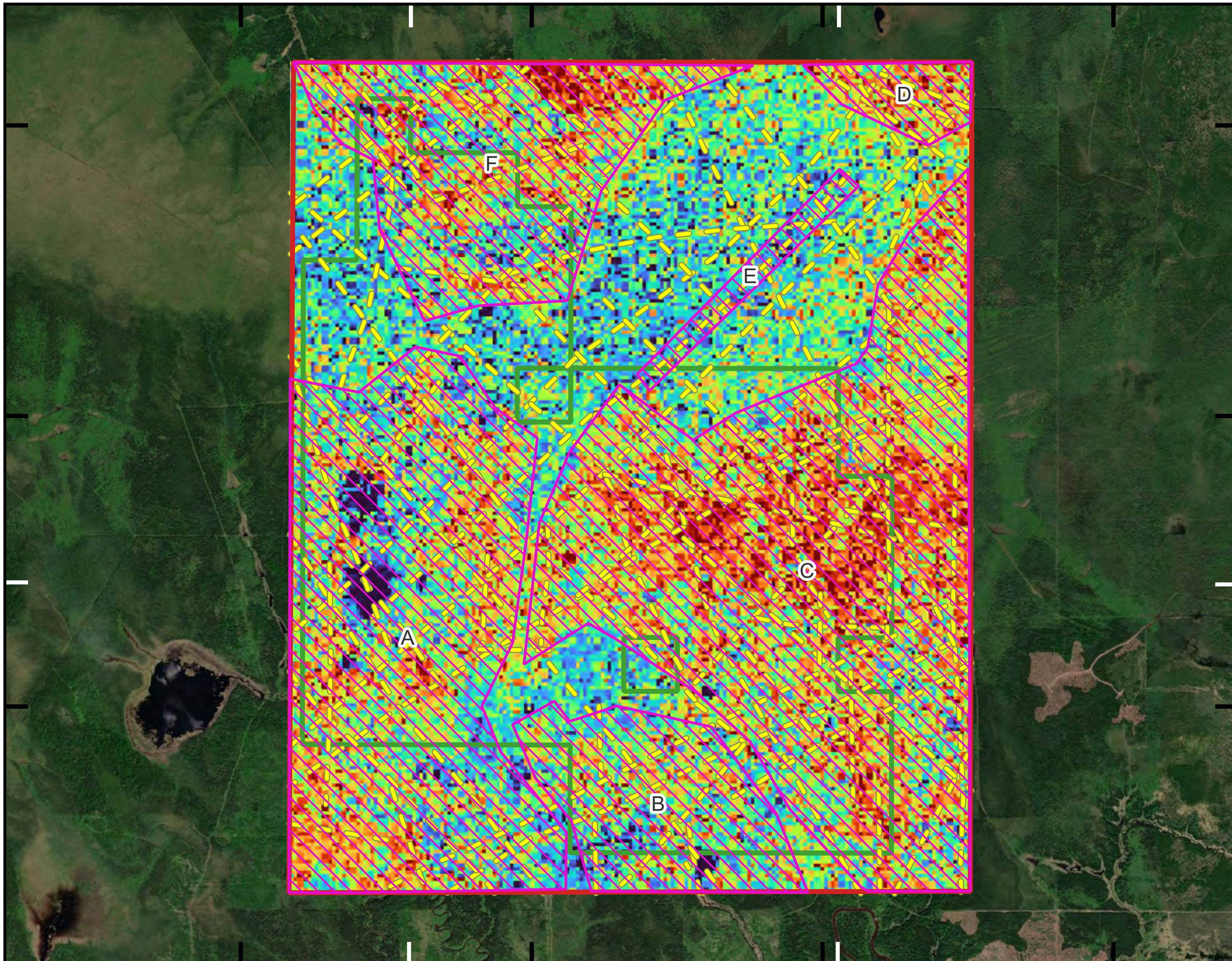

Legend

- clip_Satellite targets Gowan
- FNG Focus Areas
- clip_Surface fault traces
- Claims

ASTER

ASTER_ALUNITE_KAOLINITE_PYROPHYLLITE_S

Band 1 (Gray)

3.692294

2.934419

ESRI Satellite

0 1.5 3 Km

N

Date: January 30, 2023

CRS: WGS 84 / UTM zone 17N

Survey area with fault traces interpreted from satellite radar, multispectral processing, geophysics and available geological maps. Background is the Alunite Kaolinite Pyrophyllite Index with areas of higher signatures in Red. Interpreted targets are outlined.

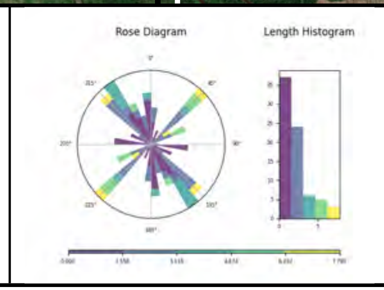

Rose diagram shows major fault strike directions. Length histogram shows length distribution of fault traces.

AXIOM APPLIED ANALYTICS

Fortune Nickel & Gold Gowan Claims - Alteration with Fault Targets

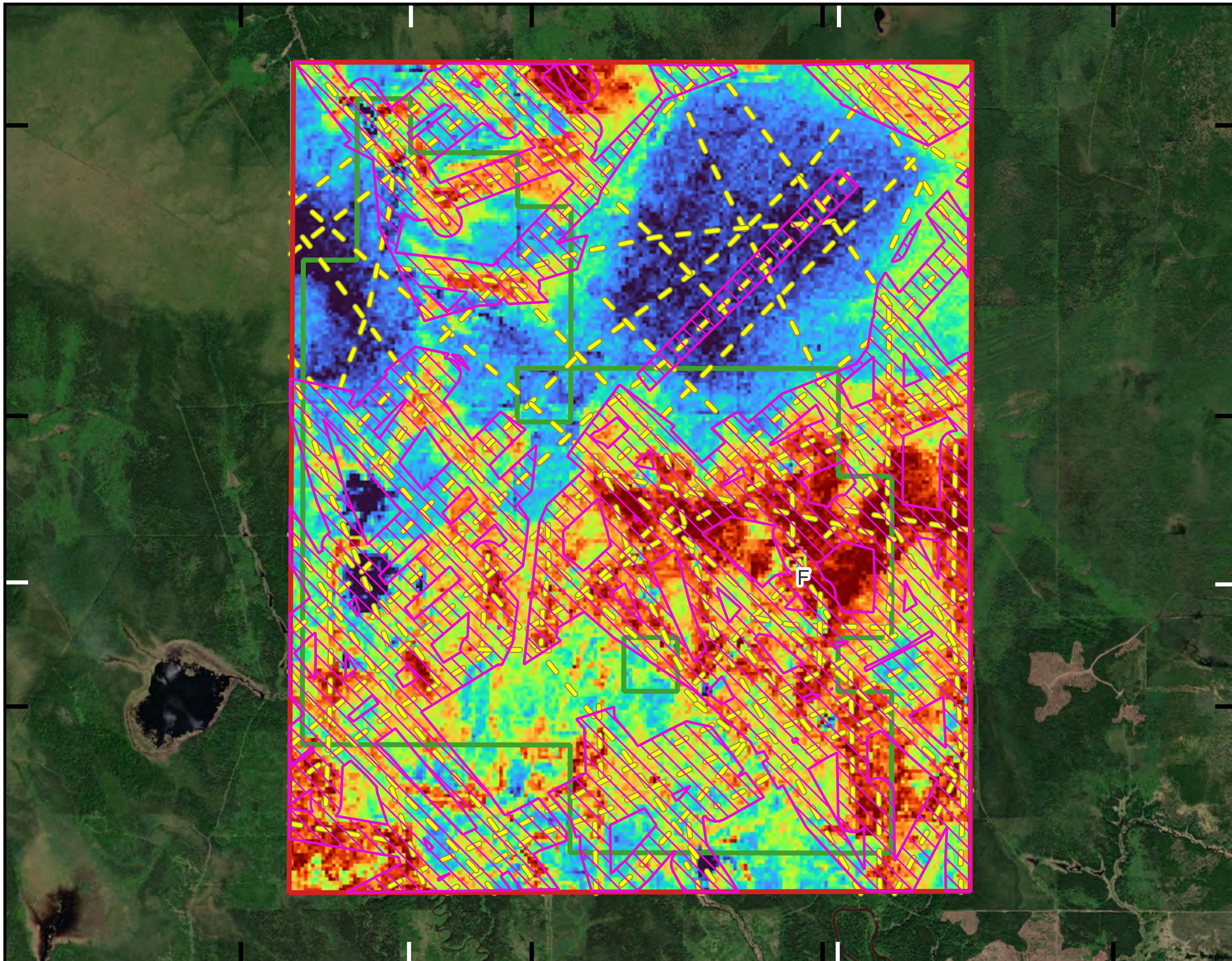

Legend

Satellite targets associated with faults and vegetation anomalies S
FNG Focus Areas
clip_Surface fault traces
Claims

ASTER

ASTER_ALTERATION2_S

Band 1 (Gray)

7.566409

4.823942

ESRI Satellite

0 1.5 3 Km

N

Date: January 30, 2023

CRS: WGS 84 / UTM zone 17N

Survey area with fault traces interpreted from satellite radar, multispectral processing, geophysics and available geological maps. Background is the Hydrothermal Alteration with areas of higher signatures in Red. Interpreted targets associated with faults are outlined.

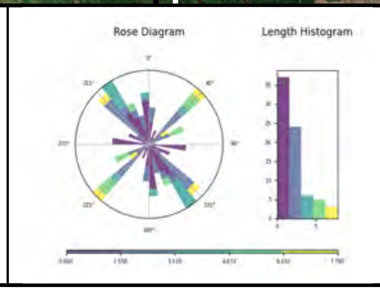

Rose diagram shows major fault strike directions. Length histogram shows length distribution of fault traces.

AXIOM APPLIED ANALYTICS

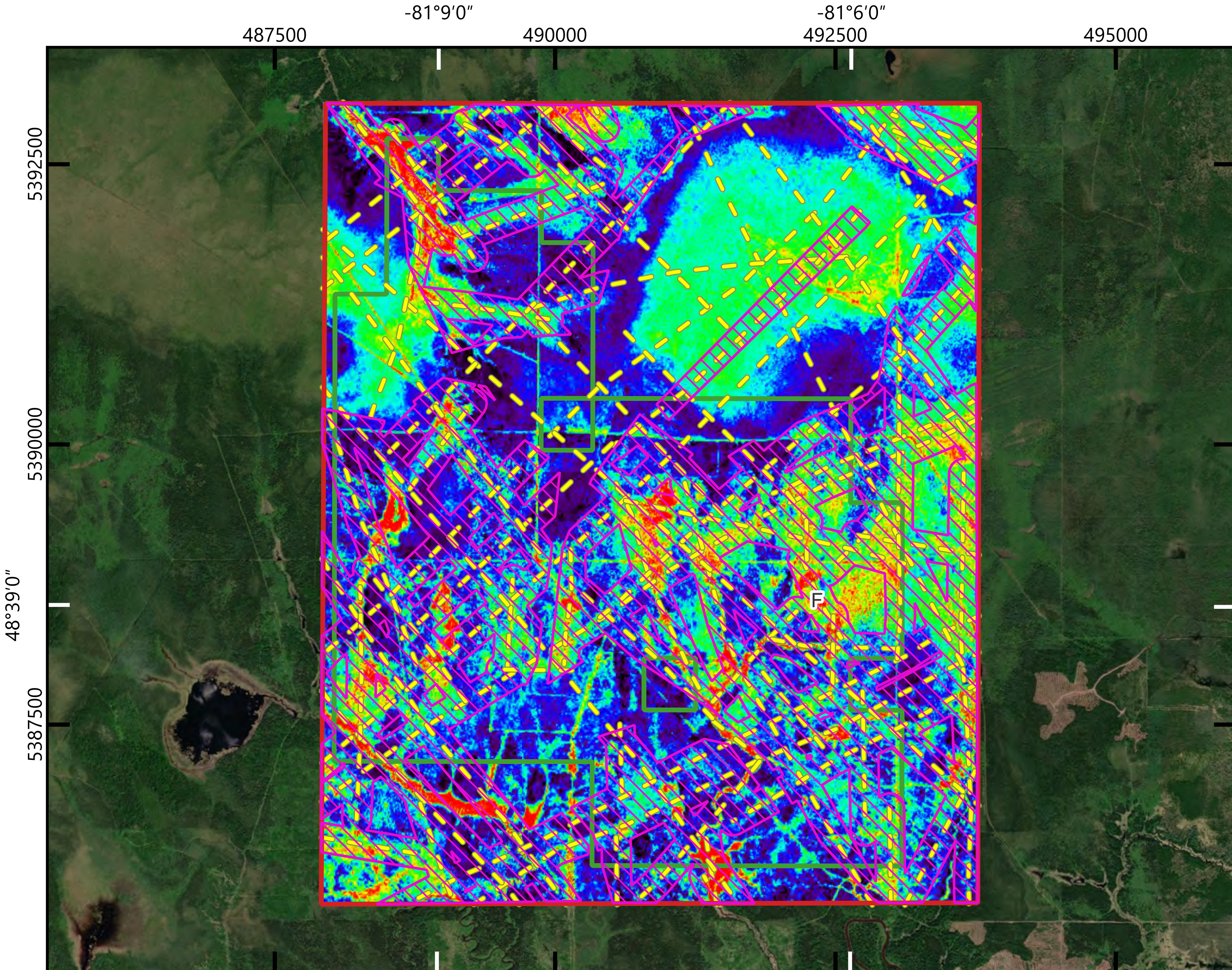

Fortune Nickel & Gold Gowan Claims - Sentinel 2 Ferric Iron

Legend

- Satellite targets associated with faults and vegetation anomalies S
- FNG Focus Areas
- clip_Surface fault traces
- Claims

S2

clip_mosaic_FNG_FERRIC IRON copy

Band 1 (Red)

High

Low

ESRI Satellite

0 1.5 3 Km

N

Date: January 30, 2023

CRS: WGS 84 / UTM zone 17N

Survey area with fault traces interpreted from satellite radar, multispectral processing, geophysics and available geological maps. Background is Ferric Iron spectra with areas of higher signatures in Red. Interpreted targets associated with faults are outlined.

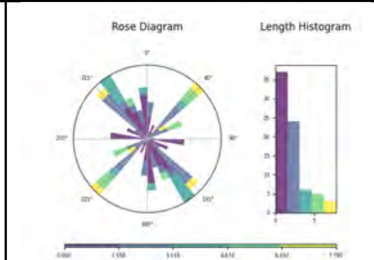

Rose diagram shows major fault strike directions. Length histogram shows length distribution of fault traces.

AXIOM APPLIED ANALYTICS

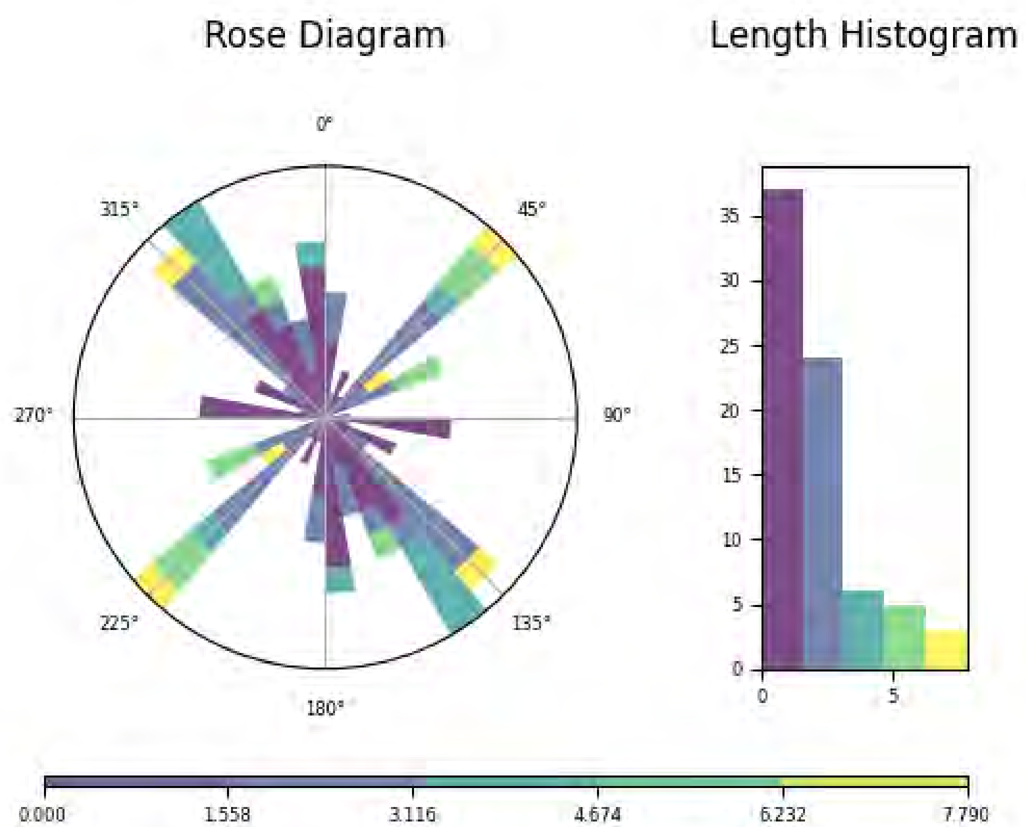

FIGURE 9: ROSE DIAGRAM FROM STRUCTURAL ANALYSIS